

1 **DEMOGRAPHY AND SELECTION SHAPE TRANSCRIPTOMIC DIVERGENCE IN**  
2 **FIELD CRICKETS**

3

4 **Running title:** evolutionary forces shaping genetic variation

5 **Keywords:** gene flow, mating behavior, *Gryllus*

6

7 **Thomas Blankers**<sup>1,2,3</sup>, **Sibelle T. Vilaça**<sup>4,5</sup>, **Isabelle Waurick**<sup>2</sup>, **David A. Gray**<sup>6</sup>, **R. Matthias Hennig**<sup>1</sup>,  
8 **Camila J. Mazzoni**<sup>4,5</sup>, **Frieder Mayer**<sup>2,7</sup>, **Emma L. Berdan**<sup>2,8</sup>

9 <sup>1</sup> *Behavioural Physiology, Department of Biology, Humboldt-Universität zu Berlin, Berlin, Germany, D-*  
10 *10115; Corresponding author: thomasblankers@gmail.com*

11 <sup>2</sup> *Museum für Naturkunde Berlin, Leibniz Institute for Evolution and Biodiversity Science, Berlin,*  
12 *Germany, D-10115*

13 <sup>3</sup> *Current Address: Department of Neurobiology and Behavior, Cornell University, Ithaca, NY, USA,*  
14 *14853*

15 <sup>4</sup> *Berlin Center for Genomics in Biodiversity Research (BeGenDiv), Berlin, Germany, D-14195*

16 <sup>5</sup> *Leibniz-Institut für Zoo- und Wildtierforschung (IZW), Berlin, Germany, D-10315*

17 <sup>6</sup> *Department of Biology, California State University Northridge, Northridge, CA, USA, 91330-8303*

18 <sup>7</sup> *Berlin-Brandenburg Institute of Advanced Biodiversity Research (BBIB), Berlin, Germany, D-14195*

19 <sup>8</sup> *Current Address: Department of Marine Sciences, University of Gothenburg, Gothenburg, Sweden, SE*  
20 *- 405 30*

21 **ACKNOWLEDGEMENTS**

22 We thank Marie Jeschek and Harald Detering from the Berlin Center for Genomics and Biodiversity  
23 (BeGenDiv) for assistance in bioinformatics. We further thank Mike Ritchie, Roger Butlin, Daniel  
24 Wegmann, and Laurent Excoffier for helpful comments on the analyses and the Biostars and  
25 Stackoverflow community for help with scripting. The manuscript strongly benefited from the comments  
26 from the associate editor Jeffrey Dudycha and three anonymous reviewers. Sample collection and  
27 processing comply with the "Principles of animal care", publication No. 86-23, revised 1985 of the  
28 National Institute of Health, and also with the current laws of Germany. The authors declare no conflict of  
29 interest. This study is part of the GENART project. The work was supported by the Leibniz Association  
30 (SAW-2012-MfN-3). STV was supported by an Alexander von Humboldt Foundation fellowship.

31 **AUTHOR CONTRIBUTIONS**

32 T.B., C.J.M, F.M, and E.L.B designed the study. T.B. and D.A.G collected the samples and I.W. did the  
33 lab work. T.B, S.T.V., and E.L.B. analysed the data. T.B and E.L.B. wrote the manuscript with  
34 contributions from R.M.H, D.A.G, and S.T.V.

35 **DATA ACCESSIBILITY**

36 Data, including raw reads, sequences used for demographic analyses and SNP data files used in outlier  
37 analysis, will be made available on Dryad and the NCBI SRA archive prior to publication.

38 **ABSTRACT**

39 Gene flow, demography, and selection can result in similar patterns of genomic variation and  
40 disentangling their effects is key to understanding speciation. Here, we assess transcriptomic variation to  
41 unravel the evolutionary history of *Gryllus rubens* and *Gryllus texensis*, cryptic field cricket species with  
42 highly divergent mating behavior. We infer their demographic history and screen their transcriptomes for  
43 footprints of selection in the context of the inferred demography. We find strong support for a long history  
44 of bidirectional gene flow, which ceased during the late Pleistocene, and a bottleneck in *G. rubens*  
45 consistent with a peripatric origin of this species. Importantly, the demographic history has likely strongly  
46 shaped patterns of neutral genetic differentiation (empirical  $F_{ST}$  distribution). Concordantly,  $F_{ST}$  based  
47 selection detection uncovers a large number of outliers, likely comprising many false positives, echoing  
48 recent theoretical insights. Alternative genetic signatures of positive selection, informed by the  
49 demographic history of the sibling species, highlighted a smaller set of loci; many of these are candidates  
50 for controlling variation in mating behavior. Our results underscore the importance of demography in  
51 shaping overall patterns of genetic divergence and highlight that examining both demography and  
52 selection facilitates a more complete understanding of genetic divergence during speciation.

53

54

## 55 INTRODUCTION

56 The study of speciation and the origins of earth's biodiversity are at the core of evolutionary biology. An  
57 important first step is understanding the mechanisms that drive genetic divergence between closely related  
58 groups of organisms. In the age of next-generation sequencing, our understanding of these mechanisms is  
59 rapidly advancing. However, a variety of processes such as gene flow, local variation in recombination  
60 and mutation rates, linked or background selection, and divergent selection often simultaneously influence  
61 genetic variation between diverging lineages and the different processes may leave similar signatures in  
62 the genome (Noor and Bennett 2009; Feder et al. 2012; Nachman and Payseur 2012; Cutter and Payseur  
63 2013; Seehausen et al. 2014; Burri et al. 2015). Therefore, to understand how populations diverge, how  
64 reproductive isolation evolves, and how this affects the genome, it is essential that we examine both  
65 selective and neutral processes.

66 Recently, the role of gene flow in speciation has drawn renewed attention (Smadja and Butlin 2011; Feder  
67 et al. 2013; Sousa and Hey 2013; Servedio 2015; Ravinet et al. 2017). It was once thought that  
68 reproductive barriers could only evolve in allopatry (Mayr 1963; Bolnick and Fitzpatrick 2007). However,  
69 this view has shifted due to accumulating evidence for varying rates of gene flow during early divergence  
70 (Bolnick and Fitzpatrick 2007; Nosil 2008; Bird et al. 2012). Although 'true' sympatric speciation is likely  
71 rare, there is nowadays a general acceptance that some amount of gene flow occurs during many  
72 speciation events, i.e. parapatric speciation (Coyne and Orr 2004; Smadja and Butlin 2011; Arnold 2015).  
73 Speciation with gene flow has attracted special attention because strong divergent selection in  
74 combination with high migration rates may lead to higher (than background) genomic divergence in the  
75 regions harboring loci important for reproductive isolation and local adaptation (Turner et al. 2005; Nosil  
76 et al. 2009; Cutter and Payseur 2013; Feder et al. 2013; Ravinet et al. 2017). However, variation in levels  
77 of divergence across the genome may also strongly depend on locally reduced intraspecific diversity due  
78 to demographic effects or variation in mutation and recombination rates (Nachman and Payseur 2012;  
79 Cruickshank and Hahn 2014; Burri et al. 2015). Additionally, the likelihood of detecting the effects of  
80 selection above background levels of genomic variation is highly dependent on the genetic architecture of

81 the traits under selection (Jiggins and Martin 2017) and the strength of selection (Ortiz-Barrientos and  
82 James 2017). These caveats warrant caution in the interpretation of the results from genomic scans,  
83 especially without a detailed understanding of the behavioral ecology and evolutionary history of the  
84 study system (Ravinet et al. 2017). Thus, a primary goal of studies aiming to elucidate the effects of  
85 selection on genetic variation should be to consider patterns left by neutral or demographic processes that  
86 could occlude the genomic signature of selection.

87 Here, we bring this goal into practice by inferring demographic history and characterizing the resulting  
88 patterns of genetic variation in the absence of selection. We then use the resulting neutral expectation to  
89 inform our inference of putative signatures of selection. For this approach, we use transcriptomic data  
90 from two sexually isolated field cricket species, *Gryllus rubens* and *Gryllus texensis*. Given their current  
91 distributions (Fig. 1), it is likely that interspecific gene flow has played a dominant role in the evolutionary  
92 history of *G. texensis* and *G. rubens*; although, contemporary gene flow is unlikely based on lack of  
93 genetic or phenotypic evidence supporting hybridization in nature (Walker 1998; Gray and Cade 2000;  
94 Higgins and Waugaman 2004) and reinforcement (Gray and Cade 2000; Izzo and Gray 2004).  
95 Additionally, a mitochondrial study found evidence that suggests *G. rubens* has a peripatric origin from *G.*  
96 *texensis* (Gray et al. 2008) and thus divergence between *G. texensis* and *G. rubens* may be associated with  
97 a strong bottleneck for the latter but not the former species.

98 In addition to demographic processes selection also likely played a role in the divergence of *G. texensis*  
99 and *G. rubens*. There is striking variation in acoustic sexual communication behavior in this system,  
100 involving multiple traits that compose the wing-generated calling song produced by cricket males and  
101 corresponding female preferences. This implies a strong selective pressure on genes related to mating  
102 signals. Variation in the cricket mating song depends on (i) the morphology and resonant properties of the  
103 wings, (ii) neural networks called central pattern generators that control rhythmic wing movement, and  
104 (iii) neuromuscular properties of the muscles that affect the temporal rhythm of the song (reviewed in  
105 Gerhardt and Huber 2002). Similarly, song recognition and preference in females are controlled by a  
106 complex network of neurons and likely depend on properties of ion channels, in particular potassium

107 channels mediating inhibitory effects (Hennig et al. 2014; Schoneich et al. 2015; Göpfert and Hennig  
108 2016). If there is indeed a strong selective pressure on mating behavior in this system, selection signatures  
109 are expected to be biased towards gene products that affect the properties of muscles, neuromuscular  
110 junctions, and neurotransmitter activity related to rhythmic behaviors and perception, as well as mating  
111 behavior variation more broadly. Importantly, combining the inference of putative selection signatures  
112 with the demographic analyses allows us to interpret the perceived effects from selection in the  
113 appropriate historical context and make predictions about the joint effects from neutral and selective  
114 forces during population divergence.

115

## 116 **MATERIALS & METHODS**

### 117 *Study system*

118 *Gryllus texensis* and *G. rubens* are widely distributed across the southern Gulf and Mid-Atlantic States in  
119 North America, with a broad sympatric region from eastern Texas through western Florida (Fig. 1). Males  
120 are morphologically cryptic (Gray et al. 2008) and there is no documented ecological divergence (Gray  
121 2011). However, females differ in the length of the ovipositor (Gray et al. 2001), which tentatively reflects  
122 ecological adaptation to different soil types (Bradford et al. 1993). In nature, divergence in acoustic  
123 signals and preferences is a strong premating barrier acting through both species-specific long-distance  
124 mate attraction songs (Walker 1998; Gray and Cade 2000; Blankers et al. 2015a) and close-range  
125 courtship songs (Gray 2005; Izzo and Gray 2011). Reproductive isolation is maintained in the zone of  
126 overlap, but there is no evidence for reproductive character displacement, indicating that reinforcement is  
127 unlikely to affect divergence in these species (Higgins and Waugaman 2004; Izzo and Gray 2004).

### 128 *Sample collection*

129 Animals were collected in the USA in Lancaster and Austin (TX; ca. 80 *G. texensis* females) and in Lake  
130 City and Ocala (FL; ca. 40 *G. rubens* females) in autumn 2013 (Fig. 1 black dots). Collected females,  
131 which are typically already inseminated in the field, were housed in containers in groups of up to 15

132 individuals with gravel substrate, shelter, and water and food *ad libitum*. Each container also contained a  
133 cup with vermiculite for oviposition. During two weeks, eggs were collected and transferred to new  
134 containers; hatchlings were then reared to adulthood. We used laboratory-raised offspring of the field-  
135 caught females between one and three weeks after their final molt rather than field-caught specimens to  
136 standardize rearing conditions across all samples. All animals (males and females) were played back an  
137 artificial stimulus resembling the conspecific male song for 10 minutes prior to sacrificing the animal. The  
138 rationale here was that one of our primary objectives was to look at genetic divergence in relation to  
139 mating behavior polymorphism. In case specific genes involved in female preference behavior were only  
140 expressed upon hearing a male song signal, this could potentially be overcome by a brief play back 30 –  
141 120 minutes prior to RNA preservation. Stimulus play back occurred for females and males to standardize  
142 the RNA sampling method across sexes. Within two hours of stimulus presentation, we sacrificed the  
143 cricket, removed the gut and then preserved the body in RNAlater following the manufacturer's  
144 instructions; samples were then stored at -80 °C until RNA isolation. A total of five males and five  
145 females were used from each of the two populations for each species (40 individuals in total; randomly  
146 sampled across containers when there were multiple containers for crickets from the same population).  
147 Total RNA extraction and directional, strand-specific Illumina library preparation were done as described  
148 in a recently published transcriptomic resource for *Gryllus rubens* (Berdan et al. 2016).

#### 149 *SNP calling*

150 Raw reads were processed using Flexbar (Dodt et al. 2012) to remove sequencing primers, adapters, and  
151 low quality bases on the 3' end of the individually barcoded reads. Samples were mapped to the *G. rubens*  
152 reference transcriptome (Berdan et al. 2016) using Bowtie2 (Langmead and Salzberg 2012) with default  
153 parameters but specifying read groups to mark reads as belonging to a specific individual. Duplicate reads  
154 were marked using 'picard' (<http://broadinstitute.github.io/picard>). The Genome Analysis Toolkit (GATK,  
155 DePristo et al. 2011; Van der Auwera et al. 2013) was used to call genotypes with the GATK-module  
156 'UnifiedGenotyper' (Van der Auwera et al. 2013). The variants were then filtered to only retain high  
157 quality SNPs based on the recommendations on the GATK website

158 (<https://gatkforums.broadinstitute.org/gatk/discussion/comment/30641>, accessed on 05/05/2015) and as  
159 described in a previous study (Berdan et al. 2015). The minor allele frequency (MAF) cut-off was set at  
160 0.025 (a minimum of two copies of the allele).

161 Our sampling design was optimized to standardize the conditions under which we stored RNA samples,  
162 but potentially introduced a bias towards collecting related individuals. This may affect both demographic  
163 inference and the summary statistics used to identify selective sweeps. To correct for the potential cryptic  
164 relatedness, we used the PLINK methods-of-moments approach (Purcell et al. 2007) implemented in the  
165 SNPrelate package (Zheng et al. 2012) in R (R Development Core Team 2016) to estimate kinship  
166 coefficients for all pairs based on the allele frequencies within each population sample. We excluded eight  
167 individuals that showed estimated kinship coefficients above 0.125 (half-sib level) with other individuals  
168 from their population, leaving 17 *G. texensis* and 15 *G. rubens* individuals for all downstream analyses.

#### 169 *The demographic history*

170 We first tested whether the sampled populations show geographic genetic structure. We inspected allele  
171 frequency variation within and between species and populations using principal component analysis. We  
172 also ran STRUCTURE (Falush et al. 2003), once for each species separately and once combining the  
173 species, using a single SNP locus per contig (8,835 randomly drawn SNPs). We used the admixture model  
174 with sampling location as prior information. We ran STRUCTURE with an MCMC chain length of  
175 100,000 and with a burn-in length of 10,000 for K=1 through K=5 (K=4 for the species-specific runs) with  
176 three repetitions for each K-value. Results were analyzed using STRUCTURE HARVESTER (Earl and  
177 vonHoldt 2012) using the log-likelihood to compare K=1 versus all other values for K and the delta K  
178 method (Evanno et al. 2005) to compare K=2 versus all higher values of K.

179 To investigate the demographic history of *G. rubens* and *G. texensis*, we used the approximate Bayesian  
180 computation framework (ABC, Beaumont *et al.* 2002). We used ABCsampler from the ABCtoolbox  
181 package (Wegmann et al. 2009) to simulate our data under different demographic scenarios in fastsimcoal  
182 v2.5.2.3 (Excoffier and Foll 2011; Excoffier et al. 2013) and to calculate summary statistics using  
183 arlsumstat v.3.5.1.3 in Arlequin v 3.5 (Excoffier and Lischer 2010). We performed the analysis using the



184 sequences from 1000 randomly drawn contigs (not including contigs with zero SNPs), using fixed  
185 recombination and mutation rates (both  $1e-8$ ) and the same minor allele frequency cut-off for the  
186 simulated data as for the observed data (0.025). To ensure that a MAF of 0.025 for the observed data was  
187 still maintained after removing the potentially related individuals, we removed all singletons that arose  
188 *post* subsampling. We initially calculated all between population summary statistics supported by  
189 arlsumstat. Then, using partial least squares regression (PLS), we retained the summary statistics with the  
190 highest predictive power (i.e. those with high factor loadings on the PLS components that significantly  
191 increase the predictive power of parameter estimates) for demographic estimates: the between-species  
192 mean and standard deviation of the number of polymorphic sites, the number of private polymorphic sites,  
193 Tajima's  $D$ , and nucleotide diversity ( $\pi$ ) in each species, as well as pairwise (between species)  $F_{ST}$  and  $\pi$ .  
194 All statistics were calculated as averages across contigs.

195 We compared four possible (groups of) models: a simple divergence model (DIV; 4 parameters for  
196 population sizes and the timing/magnitude of demographic events), three models involving gene flow  
197 (either continuous, ancient or recent gene flow/secondary contact; CGF, AGF, RGF; 6-7 parameters),  
198 three models involving a bottleneck (for either or both species; RB, TB, BB; 6-8 parameters), and a model  
199 combining the most likely gene flow and most likely bottleneck model (AGFRB; 9 parameters). We  
200 intentionally considered only relatively simple models with few parameters to avoid the risk of  
201 overparameterization (Csilléry et al. 2010). For each model, we ran 200,000 iterations to do model  
202 selection. Prior ranges for population sizes and time points were chosen on a log-uniform scale spanning  
203 across several orders of magnitude and for bottleneck size and migration rates on a uniform scale not  
204 overlapping zero (Table 1).

205 After simulating the scenarios, model selection and posterior predictive checks were performed in R.  
206 Because of their similarity, the three bottleneck models and the three gene flow models were treated as  
207 two groups of models that were first tested inter-se; the best model of each group was then tested against  
208 the DIV and best combined models. We first retained the 1% of the samples that had the smallest  
209 Euclidean distance between the summary statistics of the simulated data and the observed data (1%



210 nearest posterior samples' from hereon) for each scenario separately. We then obtained a set of linear  
211 discriminants that maximized the distance among models within the nested categories (gene flow and  
212 presence of bottleneck). Next, posterior model probabilities were calculated based on these linear  
213 combinations of summary statistics using the 'postpr' function in the 'abc' package (Csilléry et al. 2012).  
214 The first two model selection steps were used to retain one gene flow and one bottleneck model with the  
215 highest posterior probability ('best model' from hereon). A third round of model selection was used to  
216 select among a simple divergence scenario (DIV), the best gene flow and bottleneck scenarios (AGF and  
217 RB, respectively; see Results), and a scenario combining the best gene flow and the best bottleneck  
218 scenario (AGFRB). Model selection was validated by performing leave-one-out cross validation with  
219 logistic regression using the 'cv4postpr' function. Here, one simulated sample, chosen at random from the  
220 posterior distribution, is left out and considered to be the "true" model while repeating the model selection  
221 step (with the remaining posterior samples) to evaluate the robustness of the model selection (Csilléry et  
222 al. 2012).

223 To estimate demographic parameters, we then ran 1,000,000 new simulations under the model(s) with the  
224 highest posterior probability. Posterior predictive checks were performed by calculating the predicted  $R^2$   
225 and root mean squared error prediction (RMSEP) using the 'pls' package (Mevik and Wehrens 2007). We  
226 also used the 'cv4abc' function from the 'abc' package to evaluate prediction error. We estimated the  
227 demographic parameters with the 'abc' function using non-linear regression and a tolerance rate of 0.05.

228 An important goal of this study was to assess the effects of demography, in particular the timing of gene  
229 flow, on the *patterns* of transcriptome-wide genetic variation (*e.g.* the  $F_{ST}$  distribution), rather than only on  
230 summary statistics. This will provide important insight into the extent to which loci that have evolved in  
231 the absence of selection are expected to confound the signatures of selection. We thus estimated a null  
232 distribution of the allele frequency spectrum (*i.e.* Tajima's D, Tajima 1989) under the best fitting  
233 demographic model (see below). In addition, for the 1% nearest posterior samples of the models  
234 simulating continuous, recent, and ancestral gene flow and the AGFRB model we obtained the simulated

235  $F_{ST}$  distribution for each posterior sample. The median and variation of these distributions were then  
236 visually contrasted with the observed  $F_{ST}$  distribution.

### 237 *The role of selection*

238 To assess the role of selection in driving genetic divergence, we employ three approaches that differ in  
239 their sensitivity to distinguish signals of selection from the confounding effects from past demographic  
240 events. All else being equal, variation in allele frequencies between populations is expected to increase  
241 more rapidly in the presence of selection. However, the most common measure of the variance in allele  
242 frequencies among populations,  $F_{ST}$ , which is also a common test statistic to distinguish selected loci from  
243 the genomic background, has been criticized as a reliable indicator from various angles (e.g. Narum and  
244 Hess 2011; Cruickshank and Hahn 2014; Lotterhos and Whitlock 2014). Other methods may be better  
245 suited for detection of selected loci given strong demographic effects. For instance given sufficiently long  
246 divergence times and high levels primary or secondary gene flow, elevated sequence divergence ( $d_{xy}$ ) may  
247 be expected to better contrast the regions harboring loci involved in reproductive isolation from the rest of  
248 the genome (Nachman and Payseur 2012; Cruickshank and Hahn 2014). Additionally, a recent selective  
249 sweep may increase between population differentiation and decrease within population diversity and shift  
250 allele frequency spectrum (AFS) towards a higher frequency of rare alleles. Although demographic effects  
251 may also shift the AFS, these effects can be modeled and taken into account. Here, we contrast an  $F_{ST}$   
252 outlier scan (the “ $F_{ST}$  approach” from hereon) with two alternative methods that should be better suited to  
253 withstand demographic effects (hereafter “ $d_{xy}$  approach” and the “selective sweep approach”,  
254 respectively).

255 We considered loci to be potentially under positive or divergent selection if they exceeded genomic  
256 background levels of (1)  $F_{ST}$ , (2) absolute sequence divergence ( $d_{xy}$ ), or (3) frequencies of rare alleles  
257 (Tajima’s D), low diversity ( $\pi$ ), and high differentiation ( $F_{ST}$ ). For the  $F_{ST}$  approach, we used the  
258 hierarchical island model (Slatkin and Voelm 1991) implemented in Arlequin (Excoffier et al. 2009;  
259 Excoffier and Lischer 2010). To accommodate the data to Arlequin’s input file restrictions, we only  
260 considered SNPs with MAF > 5% (81,125 SNPs). We pooled the two *G. rubens* populations in one group

261 and two *G. texensis* populations in another group and performed 100,000 simulations to establish the  
262 neutral expectations for the relationship between among population heterozygosity and  $F_{ST}$ . We  
263 considered all loci with  $F_{ST}$  higher than the 99<sup>th</sup> quantile for a given level of heterozygosity to be selection  
264 outliers.

265 For the  $d_{xy}$  approach and the selective sweep approach, we used VCFtools (Danecek et al. 2011) to  
266 calculate the following summary statistics: Tajima's D (Tajima 1989), nucleotide diversity  $\pi$  (Nei and Li  
267 1979), and weighted  $F_{ST}$  (Weir and Cockerham 1984) in 1000 bp windows, and the absolute difference  
268 between the frequency of the major allele in the two species. We also calculated the average interspecific  
269 pairwise distance  $d_{xy}$  for each window as  $d_{xy} = \pi / (1 - F_{ST})$ , where  $\pi$  is the mean of the nucleotide diversity  
270 across species and  $F_{ST}$  is the weighted mean  $F_{ST}$  (Hudson et al. 1992; note that this method is similar to the  
271 often used  $d_{xy} = p_i(1-p_j) + p_j(1-p_i)$ , with  $p_i$  and  $p_j$  are the major or minor allele frequencies in species  $i$  and  
272  $j$ , averaged across windows, weighed by the number of SNPs). For the  $d_{xy}$  approach, we retained the top  
273 1% contigs with respect to  $d_{xy}$  predicting that these loci have diverged relatively early in the evolutionary  
274 history and remained shielded from gene flow throughout. For the selective sweep approach, we retained  
275 all loci that had Tajima's D below the 5% lowest simulated Tajima's D values under the inferred  
276 demographic scenario and with values for  $\pi$  and  $F_{ST}$  in the lowest and highest 10%, respectively. As this  
277 approach uses intraspecific population genetic data, we retained sets of outlier loci for both species  
278 separately

279 For all sets of outliers we checked for enriched Gene Ontology terms using 'topGO' (Alexa and  
280 Rahnenfuhrer 2016), part of the Bioconductor toolkit in R. The GO annotation was obtained from the *G.*  
281 *rubens* reference transcriptome (Berdan et al. 2016), which used the GO mapping module in Blast2Go  
282 (Conesa et al. 2005). We limited our gene set enrichment to biological process terms only and used the  
283 parent-child algorithm (Grossmann et al. 2007) to correct the  $P$  values for the 'inheritance problem' (i.e.,  
284 the problem that higher GO terms inherit annotations from more specific descendant terms leading to false  
285 positives). We considered any GO term significantly enriched if the false discovery rate (Benjamini and  
286 Hochberg 1995) associated with the corrected P-value was below 10%. To get a more detailed picture of

287 the putative functions of a given outlier locus, we looked up the functional annotation for the  
288 corresponding predicted gene product (*i.e.* the homolog with the highest similarity) on Flybase (Gramates  
289 et al. 2017) if that locus had been annotated using the *Drosophila melanogaster* proteome (see Berdan et  
290 al 2016 for details regarding transcriptome annotation).

## 291 **RESULTS**

### 292 *Transcriptomic divergence*

293 We sequenced RNA from 40 individuals (20 *G. rubens* and 20 *G. texensis*) on a HiSeq 2000 (Illumina,  
294 San Diego, CA, USA) obtaining on average 51,046,578 100-bp reads per individual (range 37,887,468-  
295 72,304,968) at a sequencing depth of eight libraries per lane. Reads mapped to the *G. rubens*  
296 transcriptome at an average rate of 83.2% (Table S1). Mapping rates were not higher in *G. rubens* despite  
297 the use of the *G. rubens* transcriptome (*G. rubens*: 83.0%; *G. texensis*: 83.0%;  $P = 0.9968$ ), but females  
298 mapped at a significantly higher rate than males (86.0% versus 79.6%;  $P < 0.0001$ ). At a MAF cut-off of  
299 0.025 we found a total of 175,244 SNPs across 8835 contigs. The average transition-transversion ratio was  
300 1.6:1. Nucleotide diversity ( $\pi$ ) was similar among *G. rubens* ( $\pi = 0.11$ ,  $\sigma_\pi = 0.14$ ) and *G. texensis* ( $\pi =$   
301 0.13,  $\sigma_\pi = 0.15$ ). Median  $D$  was 0.07 (first quantile: 0.05, third quantile 0.20) and 2.7% of the SNPs  
302 (4,828) were fixed between the species (Fig. 2A). Average Tajima's  $D$  was negative for both species, but  
303 the distribution across loci showed substantial variation (Fig. 2B, C).

### 304 *The demographic history*

305 We found no substantial evidence for genetic structure in the two populations considered within either  
306 species. The species axis was the predominant axis of variation among individuals in the Principal  
307 Component Analysis (23.93% of total SNP variation, Fig. S1A), followed by axes separating *G. texensis*  
308 (PC2, 6.13% and PC3, 4.60%) and *G. rubens* (PC4, 4.35%) individuals. Variation within species was not  
309 related to geographic locations from which the individuals were collected (Fig. S1B, C). STRUCTURE  
310 further supported the finding that neither of the species was strongly differentiated geographically. The  
311 optimal  $K$  equaled 2 when we ran STRUCTURE with both species included (Fig. S2). Examining

312 population structure within species revealed weak evidence for population substructure in both species at  
313  $K=2$ , but  $K = 1$  was the most parsimonious given the spread in log-likelihoods across  $K$ -values (Fig. S2).  
314 These results are robust across different subsets of SNPs and sample sizes (Fig. S3).  
315 To infer the role of gene flow and bottlenecks during the evolutionary history of *G. texensis* and *G.*  
316 *rubens*, we used a nested rejection procedure to select the best model out of eight different models varying  
317 in the presence and timing of bottlenecks and gene flow (Fig. 3). First, we compared the gene flow models  
318 with each other. The gene flow model with the highest posterior probability was the ‘ancestral gene flow’  
319 model (AGF  $P_{\text{posterior}} = 0.99$  versus continuous gene flow, CGF:  $P_{\text{posterior}} < 0.01$ , and recent gene flow, RGF:  
320  $P_{\text{posterior}} = 0.01$ ). Then we compared the bottleneck models with each other and found that the ‘*G. rubens*  
321 bottleneck’ model had the highest posterior probability (RB  $P_{\text{posterior}} = 0.67$  versus *G. texensis* bottleneck,  
322 TB:  $P_{\text{posterior}} = 0.43$  and both bottleneck, BB:  $P_{\text{posterior}} < 0.01$ ). We then combined these best models into a  
323 model with both ancestral gene flow and a bottleneck for *G. rubens* (AGFRB) and compared that model  
324 against a simple divergence model (DIV), the best gene flow model (AGF), and the best bottleneck model  
325 (RB). In this final model comparison, the combined model had the highest posterior probability (AGFRB:  
326  $P_{\text{posterior}} = 0.68$ ; AGF:  $P_{\text{posterior}} = 0.22$ ; DIV:  $P_{\text{posterior}} = 0.02$ ; RB:  $P_{\text{posterior}} = 0.08$ ; Fig. 3, Fig. 4). Similar  
327 results were obtained using the full sample, including additional, but potentially related individuals:  
328 AGFRB:  $P_{\text{posterior}} = 0.75$ ; AGF:  $P_{\text{posterior}} = 0.21$ ; DIV:  $P_{\text{posterior}} = 0.03$ ; RB:  $P_{\text{posterior}} = 0.01$ .  
329 As posterior probabilities may differ even among very similar models, it is critical to evaluate statistical  
330 support for model choice. Overall, model choice was well supported. For each selection step, we used  
331 cross validation to verify that models can be distinguished by assuming one of the models is the ‘true’  
332 model and then performing 1,000 independent model selection steps under that assumption. The accuracy  
333 with which the assumed ‘true’ model was chosen was high for the gene flow models (98%, 96%, and 52%  
334 for AGF, CGF, and RGF, respectively), bottleneck models (76%, 66%, and 71% of the time for RB, TB,  
335 and BB respectively), and the final model selection step (75%, 82%, 82%, 84% for DIV, AGF, RB,  
336 AGFRB, respectively). It is important to note that the AGFRB model had the highest support overall and

337 final model selection was well supported, but there is overlap of the posterior distribution of the summary  
338 statistics in multivariate space between the AGF and AGFRB models (Fig. 4).

339 Because there was some overlap between the posteriors of AGF and AGFRB (Fig. 4), and AGFRB only  
340 differs from AGF in the addition of a bottleneck, both models were used for demographic parameter  
341 estimates. Divergence times were distributed rather widely in both the AGF and AGFRB scenario and  
342 posterior density distributions were widely overlapping. The median divergence time varied between  
343 350,000 years ago (700,000 generations ago) for AGF and double that for AGFRB. The ancestral effective  
344 population size was estimated around 200,000, almost an order of magnitude higher than the model  
345 estimates for current effective population sizes in *G. rubens* (~31,000 for AGFRB and ~18,000 for AGF)  
346 and *G. texensis* (~60,000 and ~28,000; Table 1, Table S2, Fig. 6A). A bottleneck for *G. rubens* was  
347 estimated at 15% of the current effective population size (Table 1, Fig. 6C) and recovery to current  
348 population sizes was achieved around 50,000 years ago (Table 1, Fig. 6B). Ancestral gene flow was  
349 bidirectional (median  $m = 0.18$  and  $m = 0.27$  for gene flow from *G. texensis* into *G. rubens* and vice versa,  
350 respectively; Table 1, Fig. 6C) and ceased around 18,000 years ago (Table 1, Table S2, Fig. 6B). The  
351 parameter estimates for the main model, AGFRB, were robust to the inclusion of additional, but  
352 potentially related, individuals; the estimates for times and population sizes were slightly higher and the  
353 inclusion of more samples gave similar results but at slightly higher accuracy (narrower HPD interval,  
354 Table S3, Fig. S4).

355 Statistical support for parameter inference varied across demographic events. Overall, the observed  
356 summary statistics fell well within the range of the simulated multivariate summary statistics under the  
357 AGF and AGFRB models (Fig. 4) and 95% HPD intervals of the distributions were generally narrow (Fig.  
358 6, Table 1). For some demographic parameters (current population sizes for *G. rubens* [ $N_{RUB}$ ] and *G.*  
359 *texensis* [ $N_{TEX}$ ], and time since cessation of gene flow [ $T_{ISO}$ ] support was high ( $R^2 > 0.81$ ;  $RMSEP < 0.44$ );  
360 for other parameters estimated error rates were appreciably higher (Table 1, Table S2).

361 We compared  $F_{ST}$  distributions simulated under the AGF, CGF, RGF, and AGFRB models with the  
362 observed  $F_{ST}$  distribution as a measure of the effect of demography on the patterns of transcriptome-wide

363 genetic variation. We found that the observed distribution (red line in Fig. 5) closely matched the  
364 simulated distribution of the two models with ancestral gene flow for most parts, including the secondary  
365 peak at the highest  $F_{ST}$  bin ( $0.95 < F_{ST} \leq 1.00$ , Fig. 5C, D). In contrast, the observed  $F_{ST}$  distribution  
366 showed substantial mismatch with the recent and continuous gene flow models.

### 367 *The role of selection*

368 The  $F_{ST}$  approach gave by far the highest number of outlier contigs. There were 514 contigs (5.8% of  
369 contigs) that had at least one SNP designated as a selection outlier (99<sup>th</sup> quantile) in Arlequin's  $F_{ST}$  based  
370 hierarchical island method. There were no significantly (FDR < 10%) enriched Gene Ontology categories  
371 among the predicted gene products of these contigs and the most strongly enriched categories included  
372 mitochondrial processes, GTPase activity and cellular metabolism (Table S4, Table S5, Fig S5).

373 There were 80 contigs with  $d_{xy}$  values in the 99<sup>th</sup> percentile. The putative gene products corresponding to  
374 these 80 contigs were significantly (FDR < 10%) enriched for pheromone biosynthesis, hormone  
375 biosynthesis, mating behavior, and protein maturation (Table S4). Several of the most divergent loci  
376 match genes involved in *Drosophila melanogaster* sex pheromone pathways, such as  *$\alpha$ -esterase* and  
377 *Desaturase1*, mushroom body development and neuromuscular synaptic targets, such as *S-lap1*, *tartan*,  
378 including those involved in flight muscle activity (*Stretchin-Mlck*), and acoustic mating behavior, such as  
379 *Juvenile hormone esterase* and *calmodulin* (Table S6).

380 We retained 55 and 92 contigs that showed possible signatures of recent selective sweeps (Tajima's D  
381 below 5% of the simulated sequences under the AGFRB scenario and  $\pi$  and  $F_{ST}$  in the 90<sup>th</sup> percentile) in  
382 *G. texensis* and *G. rubens*, respectively. The combined set of outlier loci was not significantly enriched for  
383 any biological processes after FDR correction. The most strongly enriched GO terms were predominantly  
384 higher order GO terms such as 'organelle organization', 'primary metabolic process', and 'regulation of  
385 biological process', but also contained more specific terms: 'sperm mitochondrion organization', 'oocyte  
386 fate determination', and 'regulation of female receptivity' (Table S4). Six contigs were shared between the  
387 species-specific sets of loci that showed potential signatures of a recent selective sweep signature. Three  
388 of these have no functionally characterized gene products. The other three are *neuroglian* (*nrg*), which is



389 involved in various aspects of nervous system development and associated with male and female courtship  
390 behavior in *D. melanogaster*; *discs large 1* (*dlg1*), which affects neuromuscular junctions and changes  
391 fruit fly behavior across several domains including circadian activity and courtship; and *secretory 23*  
392 (*sec23*), which is an important component in differentiation of extra-cellular membranes in neurons and  
393 epithelial cells (Table S7). Several other gene products associated with contigs in the species- specific sets  
394 have functional roles in calcium or potassium channel activity (e.g., *nervana2*, expressed in the  
395 *Drosophila* auditory organs), nervous system development (e.g. *muscleblind*, which also alters female  
396 receptivity during courtship), veined-wing song generation (e.g. *period*), as well as many genes related to  
397 metabolic and cellular processes.

398 There was one (unannotated) contig shared between the  $d_{xy}$  approach and the selective sweep approach.  
399 Additionally, among the 514 outlier loci detected in Arlequin encompassed 11 contigs also found with the  
400  $d_{xy}$  approach, and 25 and 9 contigs respectively that were shared with the *G. rubens* and *G. texensis*  
401 specific selective sweep approach. These included the genes described above that are potentially related to  
402 sex pheromones biosynthesis (*Desat1*), flight muscle activity (*Mlc-k*), sensory neuron development (*nrg*),  
403 and auditory pathway ion channel activity (*nrv2*).

#### 404 **DISCUSSION**

405 Here, we illuminate the role of demographic and selective processes in shaping genetic variation during  
406 speciation. Combined insight in putative neutral (neutral divergence given the demographic history) and  
407 selective effects allowed us to infer the evolutionary history of *Gryllus rubens* and *G. texensis*, sibling  
408 species with large, overlapping distributions and strong phenotypic divergence in sexual traits with limited  
409 divergence in other phenotypes. We find strong support for a long history of ancestral gene flow and a  
410 bottleneck in *G. rubens*. Importantly, our data lend support to the hypothesis that loci showing high  
411 relative genetic differentiation compared to the genomic background may have evolved in response to  
412 demographic events and drift rather than in response to selection. Interestingly, several of the loci with  
413 show signatures of positive or divergent selection after taking into account the effects from demography  
414 are potential orthologs of *D. melanogaster* genes involved in premating isolation, a major source of

415 reproductive isolation between *G. rubens* and *G. texensis*. This work represents an important first step in  
416 assessing the contribution of neutral and selective forces to genetic divergence in a model system for  
417 sexual selection research.

#### 418 *Neutral divergence and demography*

419 We sequenced the transcriptomes of 40 individuals across four populations. Our observed  
420 transition:transversion ratio of 1.6:1 compares well with the estimate (1.55) from another cricket species  
421 pair, *G. firmus* and *G. pennsylvanicus* (Andrés et al. 2013), and suggests that sequencing errors did not  
422 contribute unduly to SNP discovery. Divergence across ~175K SNPs showed a bimodal and slightly right-  
423 skewed distribution of absolute (allele frequency) divergence,  $D$  (Fig. 2), and genetic differentiation,  $F_{ST}$   
424 (Fig. 5). The  $F_{ST}$  distributions simulated under our top two scenarios were also right-skewed and strongly  
425 resembled the observed distribution of genetic differentiation, in strong contrast to  $F_{ST}$  distributions  
426 corresponding to other models. Most importantly the simulated distributions under the most likely  
427 demographic scenarios, AGF and AGFRB, showed secondary peaks at  $F_{ST} > 0.95$ . This indicates that a  
428 significant proportion of our fixed loci may have risen to fixation stochastically due to neutral processes (a  
429 combination of drift, population size variation, and gene flow) while gene flow homogenizes other  
430 (random) parts of the genome. Concordantly, the  $F_{ST}$  based approach uncovered substantially more loci  
431 with putative signatures of positive selection than methods based on allele frequency spectra (with  
432 thresholds informed by inferred demographic history) or absolute sequence divergence (514 contigs in the  
433  $F_{ST}$  approach versus ~50-90 contigs in the other approaches). Our findings emphasizes the shortcomings  
434 of traditional  $F_{ST}$  outlier approaches to discern selection effects from genomic background variation  
435 (Narum and Hess 2011; Lotterhos and Whitlock 2014).

436 We find strong evidence for a long history of bidirectional gene flow before *G. rubens* and *G. texensis*  
437 became fully reproductively isolated around 18,000 years ago, sometime during the last Pleistocene  
438 glacial cycles. This finding adds to a growing body of work that suggest divergence can occur in the face  
439 of gene flow (Bolnick and Fitzpatrick 2007; Nosil 2008; Bird et al. 2012; Feder et al. 2013). A large  
440 amount of recent work has focused on the role of gene flow in speciation, especially in combination with

441 divergent or positive selection. In the genic view of speciation (Wu 2001) most areas of the genome are  
442 homogenized among populations during divergence with gene flow, and regions showing excess  
443 differentiation are thus likely protected by selection. This idea has been tested in many model systems  
444 with mixed results (Turner et al. 2005; Ellegren et al. 2012; Nosil et al. 2012; Cruickshank and Hahn  
445 2014; Burri et al. 2015; Marques et al. 2016). Recent work suggests that genomic mosaics may in fact be  
446 mostly a consequence of linked selection caused by differences in recombination rates and density of  
447 selected loci and are thus expected to be conserved in pairwise comparisons even among distantly related  
448 taxa (Nachman and Payseur 2012; Burri et al. 2015; Van Doren et al. 2017). Our results support this idea  
449 as our demographic simulations recreated heterogeneous patterns similar to our observed data. Although  
450 selection certainly contributed to transcriptome divergence in *G. rubens* and *G. texensis* our results  
451 suggest a larger role for neutral divergence shaped by the effects of migration and population size  
452 variation and echo recent insights into the importance of considering neutral divergence when interpreting  
453 potential selection effects (e.g. reviewed in Ravinet et al. 2017).

454 In addition to bi-directional gene flow, the early stages of divergence between *G. texensis* and *G. rubens*  
455 were also influenced by a substantial bottleneck in *G. rubens*. There is some overlap between the AGF (no  
456 bottleneck) and AGFRB (with a *G. rubens* bottleneck) scenarios in the simulated summary statistic  
457 distribution, but the latter has a substantially higher posterior probability and corroborates the peripatric  
458 origin for *G. rubens* hypothesized in a previous study (Gray et al. 2008). Although that study used a single  
459 mitochondrial locus, it was done with extensive geographic sampling, and both studies suggest a  
460 bottleneck for *G. rubens*. Furthermore, estimates of strong admixture between populations within species  
461 and divergence time estimates are overlapping (this study: median ~ 0.35 - 0.70 million years ago; Gray *et*  
462 *al.* study: 0.25 – 2.0 mya). Estimates for current effective population sizes (roughly between 30 and 60  
463 thousand for the AGFRB model and between 20 and 30 thousand for the AGF model) are surprisingly low  
464 given the potential census population size for *G. texensis* is in the millions (Gray et al. 2008). Potentially,  
465 the discrepancy is due to recent population expansion (Ptak and Przeworski 2002; Nadachowska-brzyska

466 et al. 2013) or variation in individual mating success (Lande and Barrowclough 1987), as is observed in  
467 wild populations of closely related species (Ritz and Köhler 2010; Rodriguez-Munoz et al. 2010).

#### 468 *The role of selection*

469 A central aim of this study was to elucidate the role of selection during divergence within the context of  
470 the inferred demographic history. The species have strongly divergent mating behaviors with no evidence  
471 for reinforcement (Gray and Cade 2000; Higgins and Waugaman 2004; Izzo and Gray 2004; Blankers et  
472 al. 2015a). Many other cricket species show similarly strong divergence in various aspects of their mating  
473 behavior and several lines of evidence from various taxa indicate that this is at least in part driven by  
474 selection (Gray and Cade 2000; Bentsen et al. 2006; Shaw et al. 2007; Bailey 2008; Thomas and Simmons  
475 2009; Oh and Shaw 2013; Blankers et al. 2017; Pascoal et al. 2017). Here, we show that the striking  
476 behavioral divergence is to some extent reflected in elevated sequence divergence of loci with putative  
477 functions in acoustic and chemical mating behavior. We find evidence that the set of loci showing the  
478 highest levels of sequence divergence are enriched for contigs bearing significant similarity to genes with  
479 known function in mating behavior in *D. melanogaster*. In addition, among the six contigs that showed  
480 evidence for a selective sweep in both species, three are potential orthologs of genes that affect  
481 neuromuscular properties in fruit flies and have effects on the flies' mating behavior. Several other  
482 species-specific outliers are potential orthologs of genes that can be tied to mating behavior variation in  
483 *Drosophila* spp.

484 Given the substantial time since divergence and the long history of gene flow, high sequence divergence is  
485 expected for loci that have experienced limited homogenizing effects from gene flow relative to the rest of  
486 the genome. The theoretical support for speciation with gene flow driven by divergence in secondary  
487 sexual characters is very thin at best (van Doorn et al. 2004; Weissing et al. 2011; Servedio 2015). Here  
488 we provide exciting and rare evidence for speciation with primary gene flow while both phenotypic (Gray  
489 and Cade 2000), quantitative genetic (Blankers et al. 2015b, 2017), and genomic analyses (this study)  
490 highlight a role for selection on (acoustic) mating behavior in driving reproductive isolation. A compelling  
491 alternative interpretation of the findings here is that the peripatric origin of *G. rubens* has allowed for an

492 initial phase of reduced gene flow; during this phase mating signals and preferences may have diverged  
493 sufficiently (aided by a founder effect following a population bottleneck) to maintain reproductive  
494 isolation during a subsequent phase of range expansion culminating into the contemporary, widespread,  
495 and largely overlapping species' distributions. More empirical studies examining the role of gene flow and  
496 selection in systems characterized by strong sexual isolation are needed to test the theoretical predictions  
497 for speciation by sexual selection. However, this study along with other recent findings in finches  
498 (Campagna et al. 2017), fresh water stickleback (Marques et al. 2017), and cichlids (Malinsky et al. 2015)  
499 provide exciting first genomic insights into the joint effects from mating behavior divergence, sexual  
500 selection, and gene flow in the earliest phases of speciation.

501 We acknowledge that there are likely to be false positives among the detected outliers, as both linked  
502 (background) selection and demographic effects are expected to confound the signatures of positive or  
503 divergent selection (Cruickshank and Hahn 2014; Ravinet et al. 2017) and *a priori* expectations also  
504 increase the risk of “storytelling” (Pavlidis et al. 2012). By using coalescent simulations under the inferred  
505 evolutionary history, we have accounted for some confounding effects from demography. However, there  
506 is still potential neutral genetic variation that is unaccounted for, most notably the potentially confounding  
507 effects of recent population expansion and variation in recombination rates. We therefore caution that  
508 there is the uncertainty associated with the results obtained here and with genomic scans on quantitative  
509 traits in general (Jiggins and Martin 2017). Nevertheless, our findings provide exciting incentive for  
510 validation using alternative methods (e.g., QTL mapping) and follow-up functional genomic analyses.

511 Unsurprisingly, not all “outlier” contigs could be linked to mating behavior. The rest of these outliers are  
512 likely comprised of three groups: (1) Loci that are physically linked to loci under selection: In the earliest  
513 phases of speciation, only loci directly under strong divergent selection will differ. However, gene  
514 frequencies at tightly linked loci will also change and, given sufficient time as well as low to moderate  
515 migration and recombination rates, these loci will be swept to fixation along with selected sites (Smith and  
516 Haigh 1974) in a process called divergence hitchhiking (Feder et al. 2012; Via 2012); (2) Loci that are  
517 under selective forces that we have not yet elucidated: It is unlikely that divergent selection only targets

518 loci involved in mating behavior and other traits may be differentiated between *G. rubens* and *G. texensis*.  
519 For example, females differ in the length of the ovipositor (Gray et al. 2001), a trait which reflects  
520 potential ecological adaptation to different soil types (Bradford et al. 1993); (3) Loci that are not under  
521 selection: Genetic drift can cause loci to drift to fixation and demographic effects such as bottlenecks and  
522 migration patterns (Holsinger and Weir 2009) can aid this process. Our simulations predict a significant  
523 number of fixed loci (1.90% on average for the AGFRB scenario) solely due to neutral processes (Fig. 5).  
524 Additionally, practical limitations of discovering low-frequency SNPs causing ascertainment bias (Clark  
525 et al. 2005) can contribute to misinterpretation of the patterns of genetic diversity (Vitti et al. 2013). A  
526 genomic map of *Gryllus* and further analyses would make strong headway into determining which of these  
527 categories the other potential outliers fall into.

528 Finally, there may be loci that are under selection but that were not detected by our scan because they  
529 simply were not being expressed. We sequenced samples from first generation laboratory offspring rather  
530 than animals directly from the field. Despite the fact that there are no differences between *G. texensis* and  
531 *G. rubens* in ecology, microhabitat use, or feeding behavior have been described (but note there is  
532 variation in the ovipositor length which is a potential adaptation to soil properties), the laboratory  
533 conditions have potentially limited our potential to detect genetic differences related to local adaptation.

534 In summary, this study underlines the importance of considering the joint effects from neutral divergence  
535 and selection in understanding the speciation process. Our results also offer unprecedented insight into the  
536 evolutionary history and the role of demography and selection in driving transcriptomic divergence in two  
537 sexually isolated field cricket sister species. We inferred that a long period of bidirectional, ancestral gene  
538 flow and a bottleneck in *G. rubens* preceded completion of reproductive isolation (Fig. 3,6). Importantly,  
539 the timing of gene flow appears to have significantly influenced the pattern of divergence (i.e. the  $F_{ST}$   
540 distribution) that we observe (Fig. 5). We also uncovered several loci that show signatures of positive or  
541 divergent selection and show that these contigs are potentially associated with courtship behavior,  
542 neuromuscular development, and chemical mating behavior. Future work will place these data on a  
543 genomic map allowing us to determine how genetic divergence is distributed relative to loci under

544 selection. These findings provide important steps towards understanding the role of selective and neutral  
545 processes in shaping patterns of divergence and the role of sexual selection during speciation-with-gene  
546 flow. They also highlight the strength of combining information on (i) the phenotypes that contribute to  
547 reproductive isolation, (ii) demographic inference, and (iii) scans for loci under selection.

#### 548 **CONFLICT OF INTEREST**

549 The authors declare no conflict of interest, financial or otherwise.

#### 550 **REFERENCES**

- 551 Alexa, A., and J. Rahnenfuhrer. 2016. topGO: Enrichment Analysis for Gene Ontology. R package  
552 version 2.30.0
- 553 Andrés, J. A., E. L. Larson, S. M. Bogdanowicz, and R. G. Harrison. 2013. Patterns of transcriptome  
554 divergence in the male accessory gland of two closely related species of field crickets. *Genetics*  
555 193:501–513.
- 556 Arnold, M. L. 2015. *Divergence with genetic exchange*. Oxford University Press.
- 557 Bailey, N. W. 2008. Love will tear you apart : different components of female choice exert contrasting  
558 selection pressures on male field crickets. *Behav. Ecol.* 19:960–966.
- 559 Beaumont, M. A., W. Zhang, and D. J. Balding. 2002. Approximate Bayesian Computation in Population  
560 Genetics. *Genetics* 162:2025–2035.
- 561 Benjamini, Y., and Y. Hochberg. 1995. Controlling the false discovery rate: a practical and powerful  
562 approach to multiple testing. *J. R. Stat. Soc. Ser. B.* 57: 289–300.
- 563 Bentsen, C. L., J. Hunt, M. D. Jennions, and R. Brooks. 2006. Complex multivariate sexual selection on  
564 male acoustic signaling in a wild population of *Teleogryllus commodus*. *Am. Nat.* 167:E102–E116.
- 565 Berdan, E. L., T. Blankers, I. Waurick, C. J. Mazzoni, and F. Mayer. 2016. A genes eye view of ontogeny:  
566 De novo assembly and profiling of a *Gryllus rubens* transcriptome. *Mol. Ecol. Resour.* 16:1478–  
567 1490.
- 568 Berdan, E. L., C. J. Mazzoni, I. Waurick, J. T. Roehr, and F. Mayer. 2015. A population genomic scan in  
569 *Chorthippus* grasshoppers unveils previously unknown phenotypic divergence. *Mol. Ecol.* 24:3918–  
570 30.
- 571 Bird, C. E., I. Fernandez-Silva, D. J. Skillings, and R. J. Toonen. 2012. Sympatric Speciation in the Post  
572 “Modern Synthesis” Era of Evolutionary Biology. *Evol. Biol.* 39:158–180.
- 573 Blankers, T., D. A. Gray, and R. M. Hennig. 2017. Multivariate Phenotypic Evolution: Divergent  
574 Acoustic Signals and Sexual Selection in *Gryllus* Field Crickets. *Evol. Biol.* 44:43–55.
- 575 Blankers, T., R. M. Hennig, and D. A. Gray. 2015a. Conservation of multivariate female preference  
576 functions and preference mechanisms in three species of trilling field crickets. *J. Evol. Biol.* 28:630–  
577 641.
- 578 Blankers, T., A. K. Lübke, and R. M. Hennig. 2015b. Phenotypic variation and covariation indicate high



- 579           evolvability of acoustic communication in crickets. *J. Evol. Biol.* 28:1656–69.
- 580 Bolnick, D. I., and B. M. Fitzpatrick. 2007. Sympatric Speciation : Models and Empirical Evidence. *Annu.*  
581           *Rev. Ecol. Evol. Syst.* 38:459–487.
- 582 Bradford, M. J., P. A. Guerette, and D. A. Roff. 1993. Testing hypotheses of adaptive variation in cricket  
583           ovipositor lengths. *Oecologia* 93:263–267.
- 584 Burri, R., A. Nater, T. Kawakami, C. F. Mugal, P. I. Olason, L. Smeds, A. Suh, L. Dutoit, S. Bures, L. Z.  
585           Garamszegi, S. Hogner, J. Moreno, A. Qvarnstrom, M. Ruzic, S. A. Saether, G. P. Saetre, J. Torok,  
586           and H. Ellegren. 2015. Linked selection and recombination rate variation drive the evolution of the  
587           genomic landscape of differentiation across the speciation continuum of *Ficedula* flycatchers.  
588           *Genome Res.* 25:1656–1665.
- 589 Campagna, L., M. Repenning, L. F. Silveira, C. S. Fontana, P. L. Tubaro, and I. J. Lovette. 2017.  
590           Repeated divergent selection on pigmentation genes in a rapid finch radiation. *Sci. Adv.* 3:e1602404.
- 591 Clark, A. G., M. J. Hubisz, C. D. Bustamante, S. H. Williamson, and R. Nielsen. 2005. Ascertainment bias  
592           in studies of human genome-wide polymorphism. *Genome Res.* 15:1496–1502.
- 593 Conesa, A., S. Götz, J. M. García-Gómez, J. Terol, M. Talón, and M. Robles. 2005. Blast2GO: A  
594           universal tool for annotation, visualization and analysis in functional genomics research.  
595           *Bioinformatics* 21:3674–3676.
- 596 Coyne, J. A., and H. A. Orr. 2004. *Speciation*. Sinauer, Sunderland, MA.
- 597 Cruickshank, T. E., and M. W. Hahn. 2014. Reanalysis suggests that genomic islands of speciation are due  
598           to reduced diversity, not reduced gene flow. *Mol. Ecol.* 23:3133–3157.
- 599 Csilléry, K., M. G. B. Blum, O. E. Gaggiotti, and O. François. 2010. Approximate Bayesian Computation  
600           (ABC) in practice. *Trends Ecol. Evol.* 25:410–418.
- 601 Csilléry, K., O. François, and M. Blum. 2012. Approximate Bayesian Computation (ABC) in R: A  
602           Vignette. 202.162.217.53 1–21.
- 603 Cutter, A. D., and B. A. Payseur. 2013. Genomic signatures of selection at linked sites: unifying the  
604           disparity among species. *Nat. Rev. Genet.* 14:262–274.
- 605 Danecek, P., A. Auton, G. Abecasis, C. A. Albers, E. Banks, M. A. DePristo, R. E. Handsaker, G. Lunter,  
606           G. T. Marth, S. T. Sherry, G. McVean, R. Durbin, and 1000 Genomes Project Analysis Group. 2011.  
607           The variant call format and VCFtools. *Bioinformatics.* 27:2156–2158.
- 608 DePristo, M. A., E. Banks, R. Poplin, K. V Garimella, J. R. Maguire, C. Hartl, A. A. Philippakis, G. del  
609           Angel, M. A. Rivas, M. Hanna, A. McKenna, T. J. Fennell, A. M. Kernytsky, A. Y. Sivachenko, K.  
610           Cibulskis, S. B. Gabriel, D. Altshuler, and M. J. Daly. 2011. A framework for variation discovery  
611           and genotyping using next-generation DNA sequencing data. *Nat. Genet.* 43:491–498.
- 612 Dodt, M., J. T. Roehr, R. Ahmed, and C. Dieterich. 2012. FLEXBAR—flexible barcode and adapter  
613           processing for next-generation sequencing platforms. *Biology.* 1:895–905.
- 614 Earl, D., and B. vonHoldt. 2012. STRUCTURE HARVESTER: a website and program for visualizing  
615           STRUCTURE output and implementing the Evanno method. *Conserv. Genet. Resour.* 4:359–361.
- 616 Ellegren, H., L. Smeds, R. Burri, P. I. Olason, N. Backström, T. Kawakami, A. Künstner, H. Mäkinen, K.  
617           Nadachowska-Brzyska, A. Qvarnström, S. Uebbing, and J. B. W. Wolf. 2012. The genomic

- 618 landscape of species divergence in *Ficedula* flycatchers. *Nature* 491: 756-760
- 619 Evanno, G., S. Regnaut, and J. Goudet. 2005. Detecting the number of clusters of individuals using the  
620 software STRUCTURE: a simulation study. *Mol. Ecol.* 14:2611–2620.
- 621 Excoffier, L., I. Dupanloup, E. Huerta-Sánchez, V. C. Sousa, and M. Foll. 2013. Robust Demographic  
622 Inference from Genomic and SNP Data. *PLoS Genet.* 9: e1003905
- 623 Excoffier, L., and M. Foll. 2011. fastsimcoal: a continuous-time coalescent simulator of genomic diversity  
624 under arbitrarily complex evolutionary scenarios. *Bioinformatics* 27:1332–1334.
- 625 Excoffier, L., T. Hofer, and M. Foll. 2009. Detecting loci under selection in a hierarchically structured  
626 population. *Heredity.* 103:285–298.
- 627 Excoffier, L., and H. E. L. Lischer. 2010. Arlequin suite ver 3.5: A new series of programs to perform  
628 population genetics analyses under Linux and Windows. *Mol. Ecol. Resour.* 10:564–567.
- 629 Falush, D., M. Stephens, and J. K. Pritchard. 2003. Inference of Population Structure Using Multilocus  
630 Genotype Data: Linked Loci and Correlated Allele Frequencies. *Genetics.* 164:1567–1587.
- 631 Feder, J. L., S. P. Egan, and P. Nosil. 2012. The genomics of speciation-with-gene-flow. *Trends Genet.*  
632 28:342–350.
- 633 Feder, J. L., S. M. Flaxman, S. P. Egan, A. A. Comeault, and P. Nosil. 2013. Geographic Mode of  
634 Speciation and Genomic Divergence. *Annu. Rev. Ecol. Evol. Syst.* 44:73–97.
- 635 Gerhardt, H. C., and F. Huber. 2002. Acoustic communication in insects and anurans. The University of  
636 Chicago Press, Chicago.
- 637 Göpfert, M. C., and R. M. Hennig. 2016. Hearing in Insects. *Annu. Rev. Entomol.* 61: 257-276
- 638 Gramates, L. S., S. J. Marygold, G. dos Santos, J.-M. Urbano, G. Antonazzo, B. B. Matthews, A. J. Rey,  
639 C. J. Tabone, M. A. Crosby, D. B. Emmert, K. Falls, J. L. Goodman, Y. Hu, L. Ponting, A. J.  
640 Schroeder, V. B. Strelets, J. Thurmond, and P. Zhou. 2017. FlyBase at 25: looking to the future.  
641 *Nucleic Acids Res.* 45:D663–D671.
- 642 Gray, D. A. 2005. Does courtship behavior contribute to species-level reproductive isolation in field  
643 crickets? *Behav. Ecol.* 16:201–206.
- 644 Gray, D. A. 2011. Speciation, divergence, and the origin of *Gryllus rubens*: behavior, morphology, and  
645 molecules. *Insects* 2:195–209.
- 646 Gray, D. A., H. Huang, and L. L. Knowles. 2008. Molecular evidence of a peripatric origin for two  
647 sympatric species of field crickets (*Gryllus rubens* and *G. texensis*) revealed from coalescent  
648 simulations and population genetic tests. *Mol. Ecol.* 17:3836–3855.
- 649 Gray, D. A., T. J. Walker, B. E. Conley, and W. H. Cade. 2001. A morphological means of distinguishing  
650 females of the cryptic field cricket species, *Gryllus rubens* and *G. texensis* (Orthoptera : Gryllidae).  
651 *Florida Entomol.* 84:314–315.
- 652 Gray, D., and W. Cade. 2000. Sexual selection and speciation in field crickets. *Proc Natl. Acad. Sci.*  
653 97:14449–14454.
- 654 Grossmann, S., S. Bauer, P. N. Robinson, and M. Vingron. 2007. Improved detection of  
655 overrepresentation of Gene-Ontology annotations with parent--child analysis. *Bioinformatics*  
656 23:3024–3031.

- 657 Hennig, R. M., K.-G. Heller, and J. Clemens. 2014. Time and timing in the acoustic recognition system of  
658 crickets. *Front. Physiol.* 5: 286-297
- 659 Higgins, L. a., and R. D. Waugaman. 2004. Sexual selection and variation: A multivariate approach to  
660 species-specific calls and preferences. *Anim. Behav.* 68:1139–1153.
- 661 Holsinger, K. E., and B. S. Weir. 2009. Genetics in geographically structured populations: defining,  
662 estimating and interpreting FST. *Nat. Rev. Genet.* 10:639–650.
- 663 Hudson, R. R., M. Slatkin, and W. P. Maddison. 1992. Estimation of levels of gene flow from DNA  
664 sequence data. *Genetics* 132:583–589.
- 665 Izzo, A. S., and D. a. Gray. 2011. Heterospecific courtship and sequential mate choice in sister species of  
666 field crickets. *Anim. Behav.* 81:259–264.
- 667 Izzo, A. S., and D. A. Gray. 2004. Cricket song in sympatry: Species specificity of song without  
668 reproductive character displacement in *Gryllus rubens*. *Ann. Entomol. Soc. Am.* 97:831–837.
- 669 Jiggins, C. D., and S. H. Martin. 2017. Glittering gold and the quest for Isla de Muerta. *J. Evol. Biol.*  
670 30:1509–1511.
- 671 Lande, R. L., and G. F. Barrowclough. 1987. Effective population size, genetic variation, and their use in  
672 population management. Pp. 87–124 *in* M. E. Soule, ed. *Viable populations for conservation*.  
673 Cambridge University Press, Cambridge, NY.
- 674 Langmead, B., and S. L. Salzberg. 2012. Fast gapped-read alignment with Bowtie 2. *Nat. Methods* 9:357–  
675 359.
- 676 Lotterhos, K. E., and M. C. Whitlock. 2014. Evaluation of demographic history and neutral  
677 parameterization on the performance of FST outlier tests. *Mol. Ecol.* 23:2178–2192.
- 678 Marques, D. A., K. Lucek, M. P. Haesler, A. F. Feller, J. I. Meier, C. E. Wagner, L. Excoffier, and O.  
679 Seehausen. 2017. Genomic landscape of early ecological speciation initiated by selection on nuptial  
680 colour. *Mol. Ecol.* 26:7–24.
- 681 Marques, D. A., K. Lucek, J. I. Meier, S. Mwaiko, C. E. Wagner, L. Excoffier, and O. Seehausen. 2016.  
682 Genomics of Rapid Incipient Speciation in Sympatric Threespine Stickleback. *PLoS Genet.* 12:1–34.
- 683 Mayr, E. 1963. *Animal Species and Evolution*. Harvard University Press.
- 684 Mevik, B.-H., and R. Wehrens. 2007. The pls Package: Principal Component and Partial Least Squares  
685 Regression in R. *J. Stat. Softw.* 18:1–24.
- 686 Nachman, M. W., and B. A. Payseur. 2012. Recombination rate variation and speciation: theoretical  
687 predictions and empirical results from rabbits and mice. *Philos. Trans. R. Soc. B Biol. Sci.* 367:409–  
688 421.
- 689 Nadachowska-brzyska, K., R. Burri, P. I. Olason, T. Kawakami, and H. Ellegren. 2013. Demographic  
690 Divergence History of Pied Flycatcher and Collared Flycatcher Inferred from Whole-Genome Re-  
691 sequencing Data. *PLoS Genet.* 9:e1003942.
- 692 Narum, S. R., and J. E. Hess. 2011. Comparison of FST outlier tests for SNP loci under selection. *Mol.*  
693 *Ecol. Resour.* 11:184–194.
- 694 Nei, M., and W.-H. Li. 1979. Mathematical model for studying genetic variation in terms of restriction  
695 endonucleases. *Proc. Natl. Acad. Sci.* 76:5269–5273.

- 696 Noor, M. A. F., and S. M. Bennett. 2009. Islands of speciation or mirages in the desert? Examining the  
697 role of restricted recombination in maintaining species. *Heredity*. 103:439–44.
- 698 Nosil, P. 2008. Speciation with gene flow could be common. *Mol. Ecol.* 17:2103–2106.
- 699 Nosil, P., D. J. Funk, and D. Ortiz-Barrientos. 2009. Divergent selection and heterogeneous genomic  
700 divergence. *Mol. Ecol.* 18:375–402.
- 701 Nosil, P., T. L. Parchman, J. L. Feder, and Z. Gompert. 2012. Do highly divergent loci reside in genomic  
702 regions affecting reproductive isolation? A test using next-generation sequence data in *Timema* stick  
703 insects. *BMC Evol. Biol.* 12:164–176
- 704 Oh, K. P., and K. L. Shaw. 2013. Multivariate sexual selection in a rapidly evolving speciation phenotype.  
705 *Proc. Roy Soc - B Biol. Sci.* 280:20130482.
- 706 Ortiz-Barrientos, D., and M. E. James. 2017. Evolution of recombination rates and the genomic landscape  
707 of speciation. *J. Evol. Biol.* 30:1519–1521.
- 708 Pascoal, S., M. Mendrok, A. J. Wilson, J. Hunt, and N. W. Bailey. 2017. Sexual selection and population  
709 divergence II. Divergence in different sexual traits and signal modalities in field crickets  
710 (*Teleogryllus oceanicus*). *Evolution*. 71:1614–1626.
- 711 Pavlidis, P., J. D. Jensen, W. Stephan, and A. Stamatakis. 2012. A critical assessment of storytelling: gene  
712 ontology categories and the importance of validating genomic scans. *Mol. Biol. Evol.* 29:3237–3248.
- 713 Ptak, S. E., and M. Przeworski. 2002. Evidence for population growth in humans is confounded by fine-  
714 scale population structure. *Trends Genet.* 18:559–563
- 715 Purcell, S., B. Neale, K. Todd-Brown, L. Thomas, M. A. R. Ferreira, D. Bender, J. Maller, P. Sklar, P. I.  
716 W. De Bakker, M. J. Daly, and others. 2007. PLINK: a tool set for whole-genome association and  
717 population-based linkage analyses. *Am. J. Hum. Genet.* 81:559–575.
- 718 R Development Core Team, R. 2016. R: A Language and Environment for Statistical Computing. R  
719 Foundation for Statistical Computing.
- 720 Ravinet, M., R. Faria, R. K. Butlin, J. Galindo, N. Bierne, M. Rafajlović, M. A. F. Noor, B. Mehlig, and  
721 A. M. Westram. 2017. Interpreting the genomic landscape of speciation: finding barriers to gene  
722 flow. *J. Evol. Biol.* 30:1450–1477.
- 723 Ritz, M. S., and G. Köhler. 2010. Natural and sexual selection on male behaviour and morphology, and  
724 female choice in a wild field cricket population: Spatial, temporal and analytical components. *Evol.*  
725 *Ecol.* 24:985–1001.
- 726 Rodriguez-Munoz, R., A. Bretman, J. Slate, C. A. Walling, and T. Tregenza. 2010. Natural and sexual  
727 selection in a wild insect population. *Science*. 79:1269–1272.
- 728 Schoneich, S., K. Kostarakos, and B. Hedwig. 2015. An auditory feature detection circuit for sound  
729 pattern recognition. *Sci. Adv.* 1:e1500325–e1500325.
- 730 Seehausen, O., R. K. Butlin, I. Keller, C. E. Wagner, J. W. Boughman, P. a Hohenlohe, C. L. Peichel, G.-  
731 P. Saetre, C. Bank, A. Brännström, A. Brelsford, C. S. Clarkson, F. Eroukhanoff, J. L. Feder, M.  
732 C. Fischer, A. D. Foote, P. Franchini, C. D. Jiggins, F. C. Jones, A. K. Lindholm, K. Lucek, M. E.  
733 Maan, D. a Marques, S. H. Martin, B. Matthews, J. I. Meier, M. Möst, M. W. Nachman, E. Nonaka,  
734 D. J. Rennison, J. Schwarzer, E. T. Watson, A. M. Westram, and A. Widmer. 2014. Genomics and  
735 the origin of species. *Nat. Rev. Genet.* 15:176–92.

- 736 Servedio, M. R. 2015. Geography, assortative mating, and the effects of sexual selection on speciation  
737 with gene flow. *Evol. Appl.* 9: 90-102
- 738 Shaw, K. L., Y. M. Parsons, and S. C. Lesnick. 2007. QTL analysis of a rapidly evolving speciation  
739 phenotype in the Hawaiian cricket *Laupala*. *Mol. Ecol.* 16:2879–2892.
- 740 Slatkin, M., and L. Voelm. 1991. FST in a hierarchical island model. *Genetics* 127:627–629.
- 741 Smadja, C. M., and R. K. Butlin. 2011. A framework for comparing processes of speciation in the  
742 presence of gene flow. *Mol. Ecol.* 20:5123–5140.
- 743 Smith, J. M., and J. Haigh. 1974. The hitch-hiking effect of a favourable gene. *Genet. Res.* 23:23–35.
- 744 Sousa, V., and J. Hey. 2013. Understanding the origin of species with genome-scale data : modelling gene  
745 flow. *Nat. Rev. Genet.* 14:404–414.
- 746 Tajima, F. 1989. Statistical method for testing the neutral mutation hypothesis by DNA polymorphism.  
747 *Genetics* 123:585–595.
- 748 Thomas, M. L., and L. W. Simmons. 2009. Sexual selection on cuticular hydrocarbons in the Australian  
749 field cricket, *Teleogryllus oceanicus*. *BMC Evol. Biol.* 9:162–174
- 750 Turner, T. L., M. W. Hahn, and S. V. Nuzhdin. 2005. Genomic islands of speciation in *Anopheles*  
751 *gambiae*. *PLoS Biol.* 3:1572–1578.
- 752 Van der Auwera, G. A., M. O. Carneiro, C. Hartl, R. Poplin, G. del Angel, A. Levy-Moonshine, T. Jordan,  
753 K. Shakir, D. Roazen, J. Thibault, E. Banks, K. V Garimella, D. Altshuler, S. Gabriel, and M. A.  
754 DePristo. 2013. From FastQ Data to High-Confidence Variant Calls: The Genome Analysis Toolkit  
755 Best Practices Pipeline. *Curr. Protoc. Bioinformatics.* 43:1–11.
- 756 van Doorn, G. S., U. Dieckmann, and F. J. Weissing. 2004. Sympatric Speciation by Sexual Selection : A  
757 Critical Reevaluation. *Am. Nat.* 163:709–725.
- 758 Van Doren, B. M., L. Campagna, B. Helm, J. C. Illera, I. J. Lovette, and M. Liedvogel. 2017. Correlated  
759 patterns of genetic diversity and differentiation across an avian family. *Mol. Ecol.* 26:3982–3997.
- 760 Via, S. 2012. Divergence hitchhiking and the spread of genomic isolation during ecological speciation-  
761 with-gene-flow. *Philos. Trans. R. Soc. B Biol. Sci.* 367:451–460.
- 762 Vitti, J. J., S. R. Grossman, and P. C. Sabeti. 2013. Detecting Natural Selection in Genomic Data. *Annu.*  
763 *Rev. Genet* 47:97–120.
- 764 Walker, T. 1998. Trilling field crickets in a zone of overlap (Orthoptera: Gryllidae: Gryllus). *Ann.*  
765 *Entomol. Soc. Am.* 91:175–184.
- 766 Wegmann, D., C. Leuenberger, and L. Excoffier. 2009. Using ABCtoolbox.
- 767 Weir, B. S., and C. C. Cockerham. 1984. Estimating F-statistics for the analysis of population structure.  
768 *Evolution.* 38:1358–1370.
- 769 Weissing, F. J., P. Edelaar, and G. S. van Doorn. 2011. Adaptive speciation theory: a conceptual review.  
770 *Behav. Ecol. Sociobiol.* 65:461–480.
- 771 Wu, C. I. 2001. The genic view of the process of speciation. *J. Evol. Biol.* 14:851–865.



772 Zheng, X., D. Levine, J. Shen, S. Gogarten, C. Laurie, and B. Weir. 2012. A High-performance  
773 Computing Toolset for Relatedness and Principal Component Analysis of SNP Data. *Bioinformatics*  
774 28:3326–3328.

775

## 776 DATA ACCESSIBILITY

777 Data, including raw reads, sequences used for demographic analyses and SNP data files used in outlier  
778 analysis, will be made available on Dryad and the NCBI SRA archive prior to publication.

779

## 780 FIGURE LEGENDS

781 Fig. 1. Geographic distributions for *G. texensis* (red) and *G. rubens* (blue). The sympatric zone is marked  
782 with turquoise. The distributions are approximate and based on the Singing Insects of North America data  
783 base (<http://entnemdept.ufl.edu/Walker/buzz/>). The black dots in Texas and Florida represent the sampling  
784 locations for *G. texensis* and *G. rubens*, respectively.

785

786 Fig. 2. Genomic divergence. The distribution of the interspecific allele frequency difference,  $D$ , across  
787 SNPs (A), of the absolute divergence,  $d_{xy}$ , in 1000 bp windows (B), and of Tajima's  $D$  in 1000 bp  
788 windows for *G. rubens* (C) and *G. texensis* (D), respectively

789

790 Fig. 3. Demographic scenarios for Approximate Bayesian Computation. Eight scenarios were simulated  
791 under the ABC framework. (A) A simple divergence scenario (DIV) with a log uniform prior on the  
792 divergence time ( $T_{\text{SPLIT}}$ ), the ancestral population size ( $N_{\text{ANC}}$ ) and the current effective population sizes for  
793 *G. rubens* and *G. texensis* ( $N_{\text{RUB}}$ ,  $N_{\text{TEX}}$ ). (B) Three different gene flow models with either continuous gene  
794 flow (CGF), ancestral gene flow (AGF), or recent gene flow (secondary contact; RGF) were additionally  
795 defined by parameters describing migration rates ( $M_{\text{TEX} \gg \text{RUB}}$ ,  $M_{\text{RUB} \gg \text{TEX}}$ ; uniform priors not overlapping  
796 zero) and the time point since cessation of gene flow ( $T_{\text{ISO}}$ ) or of secondary contact ( $T_{\text{CONT}}$ ), both with log  
797 uniform priors. (C) Three bottleneck models defined by the time since recovery to current population sizes  
798 ( $T_{\text{BOT}}$ ; log uniform prior) and the relative population size reduction (BOTSIZE; uniform prior not  
799 overlapping zero) for *G. rubens* (RB), *G. texensis* (TB), or both (BB). (D) An additional model (AGFRB)  
800 combining the best gene flow (AGF) and best bottleneck (RB) model, marked by the black, dashed  
801 rectangles. The posterior probabilities for model selection are given left of the square (opening) brackets  
802 for the three gene flow and the three bottleneck models, and right of the square (closing) brackets for the  
803 final model selection step.

804

805 Fig. 4. Distribution of observed and simulated data sets in multivariate summary statistic space. For each  
806 of the four models used in the final model selection step (see also Fig. 3) the distribution of the 1%  
807 posterior samples with the smallest Euclidean distance to the observed data is shown relative to the  
808 coordinates of the observed data. The multivariate summary statistic space is constrained by the first two  
809 linear discriminants representing linear combinations of the summary statistics used in model selection  
810 (see text for details).

811

812 Fig. 5.  $F_{ST}$  distributions of simulated and observed data. The distribution of Weir and Cockerham's  $F_{ST}$  as  
813 calculated by the program arlsumstat are shown for 2,000 simulated data sets for different demographic  
814 model: recent gene flow (secondary contact; RGF), continuous gene flow (CGF), ancestral gene flow  
815 (AGF), and the AGFRB model. Observed data (1,000 1kbp sequences) are represented by the red solid

816 line. The histograms show the density (y-axis) to enhance comparison between simulated and observed  
817 data.

818  
819 Fig. 6. Demographic parameter estimation. For the AGFRB (A-C) and the AGF (D-F) models, the density  
820 distribution of the ancestral and current population sizes (A, D), the time since divergence, cessation of  
821 gene flow, and recovery to current population sizes after the bottleneck (B, E), and the migration rates and  
822 bottleneck size (C, F) are shown. The density lines have been trimmed to the existent parameter  
823 distribution (i.e., no density extrapolation) and have been smoothed by adjusting the bandwidth. For lines  
824 within one panel the same smoothing bandwidth has been used.

825

826 **SUPPLEMENTARY INFORMATION**

827 Table S1. Individual RNA-seq read mapping statistics

828 Table S2. ABC estimates for the AGF scenario

829 Table S3. ABC estimates for the full sample (including 8 individuals from half-sib pairs), AGFRB  
830 scenario

831 Table S4. GO enrichment results for  $F_{ST}$ ,  $d_{xy}$ , and selective sweep outliers.

832 Table S5.  $F_{ST}$  outlier loci.

833 Table S6.  $d_{xy}$  outlier loci

834 Table S7A,B Selective sweep outlier loci for *G. texensis* and *G. rubens*

835 Fig S1-S7. See figures for figure legends.

836

837 Table 1. ABC estimates. Prior distributions (log-scale), posterior predictive checks and posterior  
838 parameter estimates (log scale, median and 95% highest posterior density interval) for the model are  
839 shown.

Parameter	Prior <sup>a</sup>		Validation		Posterior		
	minimum	maximum	R <sup>2</sup>	RMSEP	2.5%	Median	97.5%
LOG <sub>10</sub> (N <sub>ANC</sub> )	4.0	6.0 (lu)	0.13	0.93	4.68	5.34	5.99
LOG <sub>10</sub> (N <sub>RUB</sub> )	3.0	6.0 (lu)	0.90	0.32	4.03	4.50	4.70
LOG <sub>10</sub> (N <sub>TEX</sub> )	3.0	6.0 (lu)	0.75	0.50	4.51	4.78	4.87
LOG <sub>10</sub> (T <sub>SPLIT</sub> ) <sup>b</sup>	5.0	7.0 (lu)	0.02	0.99	4.86	6.19	7.16
LOG <sub>10</sub> (T <sub>ISO</sub> ) <sup>b</sup>	3.0	7.0 (lu)	0.90	0.32	4.20	4.55	4.76
LOG <sub>10</sub> (T <sub>BOT</sub> ) <sup>b</sup>	5.0	7.0 (lu)	0.48	0.72	4.42	5.01	6.16
BOTSIZE	0.01	0.5 (u)	0.16	0.91	-0.04	0.15	0.48
M <sub>TEX&gt;&gt;RUB</sub>	0.01	0.5 (u)	0.06	0.97	0.01	0.18	0.54
M <sub>RUB&gt;&gt;TEX</sub>	0.01	0.5 (u)	0.06	0.97	0.01	0.27	0.74

840 <sup>a</sup> priors are uniformly (u) or log-uniformly (lu) distributed and do not overlap zero for migration rates  
841 and bottleneck size.

842 <sup>b</sup> the timing of demographic events is in (logarithm of) number of generation and both species have two  
843 generations annually.

844

845

846



847 Table S1. Individual RNA-seq read mapping statistics. Mapping rates were calculated using bowtie2 with  
848 default parameters.

Sample ID	Species	Population	Sex	Mapping rate
30037 rub	<i>G. rubens</i>	Ocala	f	84.52%
30038 rub	<i>G. rubens</i>	Ocala	f	85.33%
30039 rub	<i>G. rubens</i>	Ocala	f	85.66%
30040 rub	<i>G. rubens</i>	Ocala	f	84.35%
30041 rub	<i>G. rubens</i>	Ocala	f	84.85%
30057 rub	<i>G. rubens</i>	Lake City	f	88.40%
30059 rub	<i>G. rubens</i>	Lake City	f	88.86%
30060 rub	<i>G. rubens</i>	Lake City	f	87.83%
30061 rub	<i>G. rubens</i>	Lake City	f	90.23%
30052 rub	<i>G. rubens</i>	Ocala	m	78.01%
30053 rub	<i>G. rubens</i>	Ocala	m	80.72%
30055 rub	<i>G. rubens</i>	Ocala	m	79.76%
30063 rub	<i>G. rubens</i>	Lake City	m	77.70%
30064 rub	<i>G. rubens</i>	Lake City	m	77.56%
30065 rub	<i>G. rubens</i>	Lake City	m	70.75%
30027 tex	<i>G. texensis</i>	Lancaster	f	83.09%
30028 tex	<i>G. texensis</i>	Lancaster	f	83.20%
30029 tex	<i>G. texensis</i>	Lancaster	f	81.61%
30030 tex	<i>G. texensis</i>	Lancaster	f	83.80%
30031 tex	<i>G. texensis</i>	Lancaster	f	80.42%
30043 tex	<i>G. texensis</i>	Austin	f	91.78%
30044 tex	<i>G. texensis</i>	Austin	f	90.01%
30046 tex	<i>G. texensis</i>	Austin	f	87.70%
30032 tex	<i>G. texensis</i>	Lancaster	m	76.17%
30033 tex	<i>G. texensis</i>	Lancaster	m	77.76%
30034 tex	<i>G. texensis</i>	Lancaster	m	77.24%
30035 tex	<i>G. texensis</i>	Lancaster	m	80.79%
30036 tex	<i>G. texensis</i>	Lancaster	m	76.77%
30047 tex	<i>G. texensis</i>	Austin	m	86.40%
30049 tex	<i>G. texensis</i>	Austin	m	88.52%
30050 tex	<i>G. texensis</i>	Austin	m	79.15%
30051 tex	<i>G. texensis</i>	Austin	m	86.18%

849  
850  
851  
852  
853  
854

855 Table S2. ABC estimates for the AGF scenario. Prior distributions (log-scale), posterior predictive checks  
 856 and posterior parameter estimates (log scale, median and 95% highest posterior density interval) for the  
 857 model are shown.

Parameter	Prior <sup>a</sup>		Validation		Posterior		
	minimum	maximum	R <sup>2</sup>	RMSEP	2.5%	Median	97.5%
LOG <sub>10</sub> (N <sub>ANC</sub> )	4.0	6.0 (lu)	0.0	0.96	4.76	5.31	5.81
LOG <sub>10</sub> (N <sub>RUB</sub> )	3.0	6.0 (lu)	0.93	0.27	3.81	4.26	4.55
LOG <sub>10</sub> (N <sub>TEX</sub> )	3.0	6.0 (lu)	0.93	0.27	3.98	4.45	4.69
LOG <sub>10</sub> (T <sub>SPLIT</sub> ) <sup>b</sup>	5.0	7.0 (lu)	0.06	0.97	4.61	5.83	7.04
LOG <sub>10</sub> (T <sub>ISO</sub> ) <sup>b</sup>	3.0	7.0 (lu)	0.79	0.46	4.21	4.56	4.73
M <sub>TEX&gt;&gt;RUB</sub>	0.01	0.5 (u)	0.17	0.91	0.03	0.24	0.49
M <sub>RUB&gt;&gt;TEX</sub>	0.01	0.5 (u)	0.12	0.94	0.01	0.26	0.51

858 <sup>a</sup> priors are uniformly (u) or log-uniformly (lu) distributed and do not overlap zero for migration rates  
 859 and bottleneck size.

860 <sup>b</sup> the timing of demographic events is in (logarithm of) number of generation and both species have two  
 861 generations annually.

862  
 863 Table S3 ABC estimates for the full sample (including 8 individuals from half-sib pairs), AGFRB  
 864 scenario. Prior distributions (log-scale), posterior predictive checks and posterior parameter estimates (log  
 865 scale, median and 95% highest posterior density interval) for the model are shown.

Parameter	Prior <sup>a</sup>		Validation		Posterior		
	minimum	maximum	R <sup>2</sup>	RMSEP	2.5%	Median	97.5%
LOG <sub>10</sub> (N <sub>ANC</sub> )	4.0	6.0 (lu)	0.05	0.974	4.94	5.32	5.72
LOG <sub>10</sub> (N <sub>RUB</sub> )	3.0	6.0 (lu)	0.89	0.333	4.70	4.79	4.87
LOG <sub>10</sub> (N <sub>TEX</sub> )	3.0	6.0 (lu)	0.88	0.346	4.73	4.85	4.94
LOG <sub>10</sub> (T <sub>SPLIT</sub> ) <sup>b</sup>	5.0	7.0 (lu)	0.01	0.997	5.49	6.23	6.74
LOG <sub>10</sub> (T <sub>ISO</sub> ) <sup>b</sup>	3.0	7.0 (lu)	0.81	0.438	4.27	4.53	4.72
LOG <sub>10</sub> (T <sub>BOT</sub> ) <sup>b</sup>	5.0	7.0 (lu)	0.02	0.990	5.14	5.19	5.32
BOTSIZE	0.01	0.5 (u)	0.01	0.995	0.09	0.15	0.23
M <sub>TEX&gt;&gt;RUB</sub>	0.01	0.5 (u)	0.12	0.938	0.05	0.12	0.18
M <sub>RUB&gt;&gt;TEX</sub>	0.01	0.5 (u)	0.12	0.938	0.01	0.18	0.75

866 <sup>a</sup> priors are uniformly (u) or log-uniformly (lu) distributed and do not overlap zero for migration rates  
 867 and bottleneck size.

868 <sup>b</sup> the timing of demographic events is in (logarithm of) number of generation and both species have two  
 869 generations annually.

870

871

872

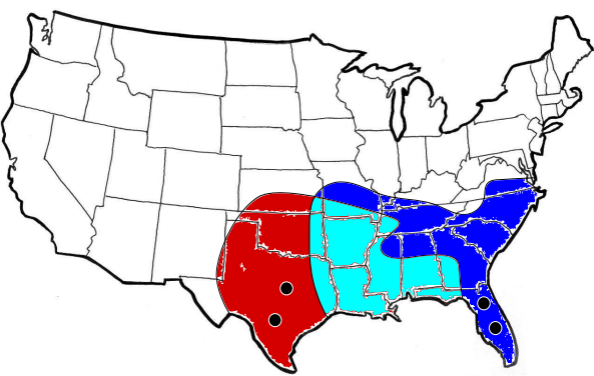
873 Table S4. GO enrichment results. The top ten terms of the Gene Ontology enrichment is shown for the  $d_{xy}$   
 874 outliers and the Allele Frequency Spectrum (AFS) outliers. For each Biological Process, the number of  
 875 annotated transcripts and the number of observed and expected transcripts in the sample with a given  
 876 annotation are shown. The Fisher's exact test P-value is corrected using the parent-child algorithm  
 877 (Grossmann *et al.* 2007). The FDR is the false discovery rate based on the corrected P-values.  
 878

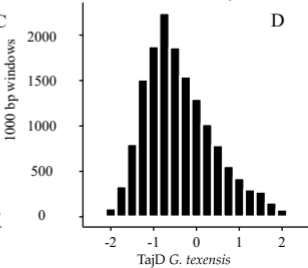
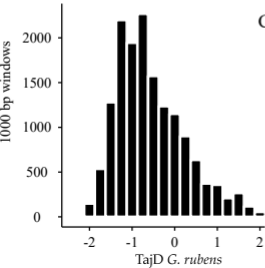
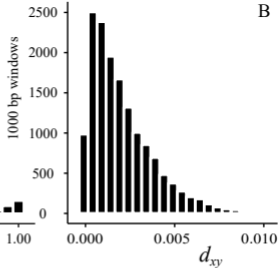
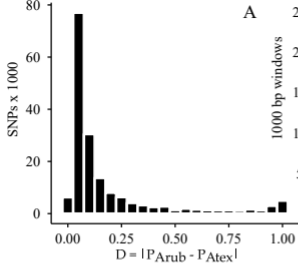
GO	Term	#Annot	#Sample	#Exp	P-value	FDR
		<b><i>Fsr</i></b>				
GO:0032543	mitochondrial translation	10	4	0.34	0.00056	1
GO:0043087	regulation of GTPase activity	54	10	1.85	0.00123	1
GO:0071695	anatomical structure maturation	2	2	0.07	0.00141	1
GO:0010822	positive regulation of mitochondrion organization	5	3	0.17	0.0026	1
GO:0044267	cellular protein metabolic process	1773	74	60.58	0.00318	1
GO:0022411	cellular component disassembly	56	7	1.91	0.00398	1
GO:0000910	cytokinesis	248	19	8.47	0.00428	1
GO:0043603	cellular amide metabolic process	577	30	19.72	0.00526	1
GO:0030716	oocyte fate determination	58	6	1.98	0.00564	1
GO:0050789	regulation of biological process	4028	160	137.63	0.00566	1
		<b><math>d_{xy}</math></b>				
GO:0042811	pheromone biosynthetic process	44	4	0.2	4.30E-06	0.0027
GO:0042810	pheromone metabolic process	49	4	0.22	3.60E-05	0.0071
GO:1903317	regulation of protein maturation	24	3	0.11	3.70E-05	0.0071
GO:0042446	hormone biosynthetic process	82	4	0.37	4.50E-05	0.0071
GO:1903318	negative regulation of protein maturation	23	3	0.1	0.0001	0.0152
GO:0044705	multi-organism reproductive behavior	359	6	1.62	0.0002	0.0232
GO:0019098	reproductive behavior	367	6	1.65	0.0005	0.0380
GO:0007618	mating	400	6	1.8	0.0005	0.0380
GO:0006551	leucine metabolic process	3	2	0.01	0.0011	0.0734
		<b>AFS</b>				
GO:0006996	organelle organization	2271	41	21.7	0.0003	0.3545
GO:1902589	single-organism organelle organization	1791	32	17.1	0.0004	0.3545
GO:0044238	primary metabolic process	4836	59	46.2	0.0007	0.4181
GO:0090066	regulation of anatomical structure size	375	12	3.6	0.0014	0.5867
GO:0050789	regulation of biological process	4028	52	38.5	0.0025	0.5867
GO:0030382	sperm mitochondrion organization	6	2	0.1	0.0027	0.5867
GO:0065007	biological regulation	4463	56	42.7	0.0027	0.5867
GO:0007294	germarium-derived oocyte fate determination	46	4	0.4	0.0028	0.5867
GO:0030716	oocyte fate determination	58	4	0.6	0.0033	0.5867
GO:0045924	regulation of female receptivity	7	2	0.1	0.0035	0.5867
GO:0006996	organelle organization	2271	41	21.7	0.0003	0.3545

879  
 880  
 881  
 882

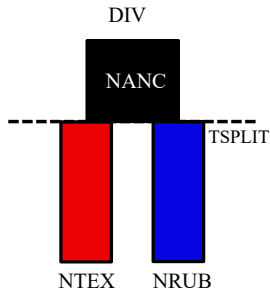
883

884

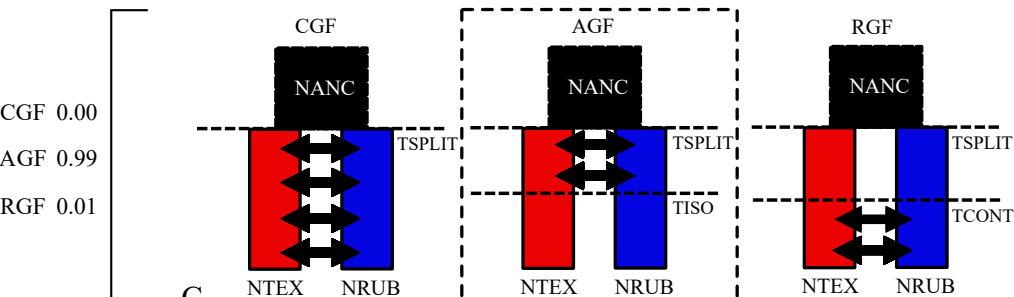




A



B

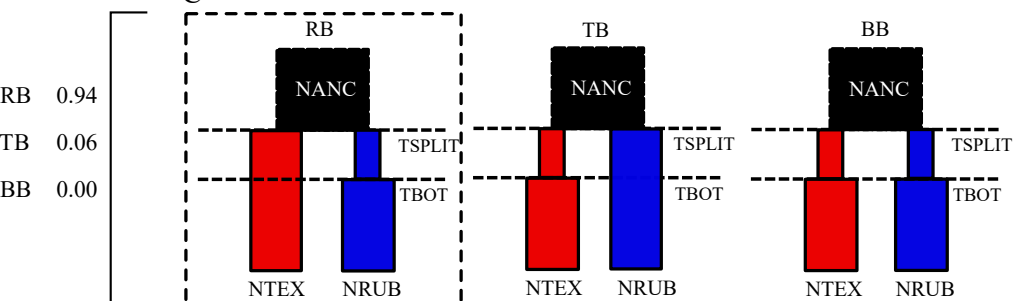


CGF 0.00

AGF 0.99

RGF 0.01

C

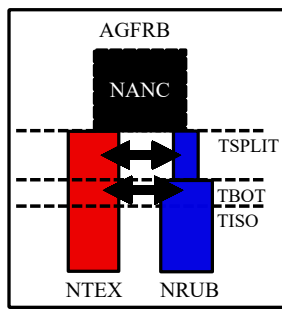


RB 0.94

TB 0.06

BB 0.00

D



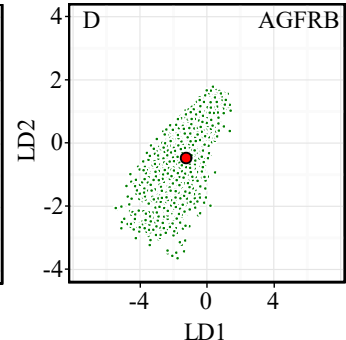
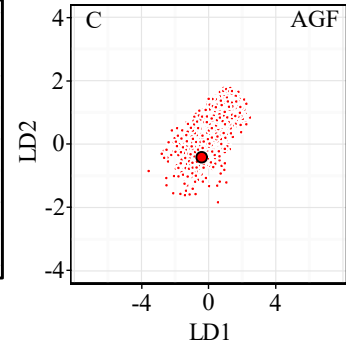
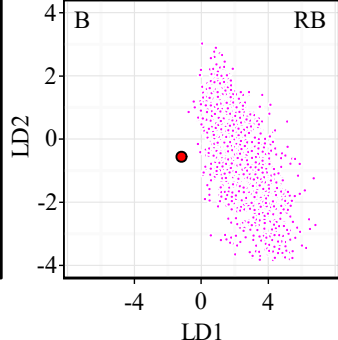
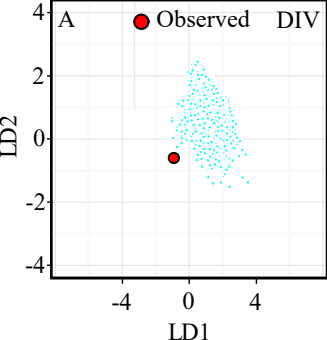
DIV 0.00

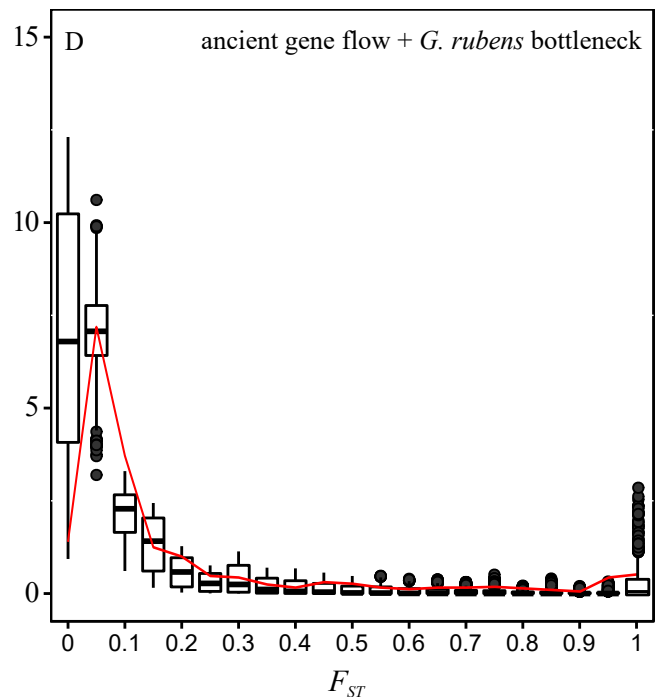
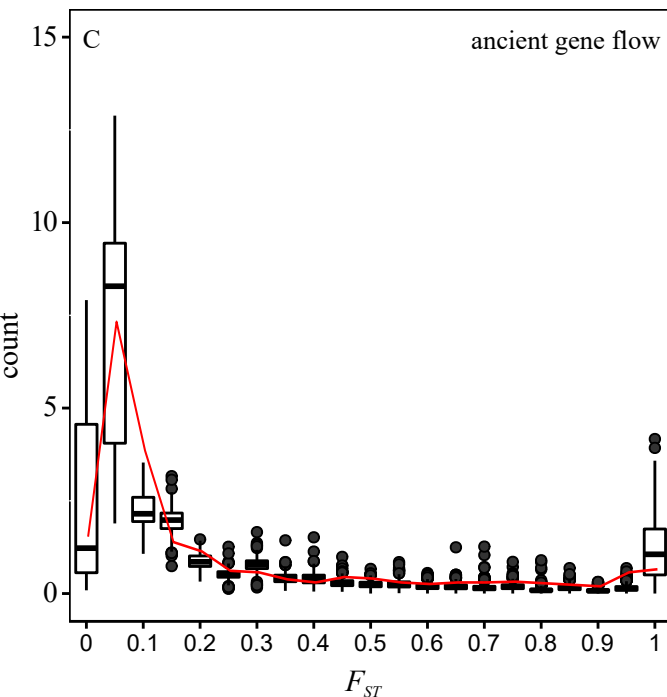
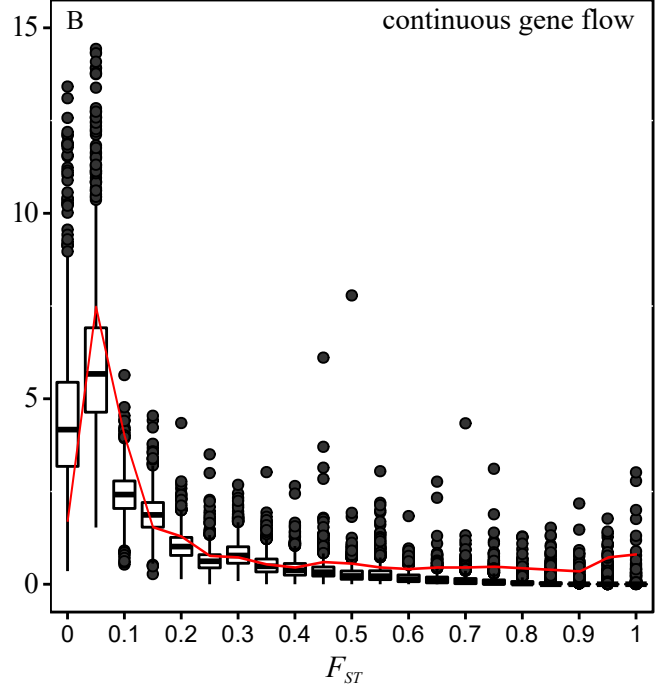
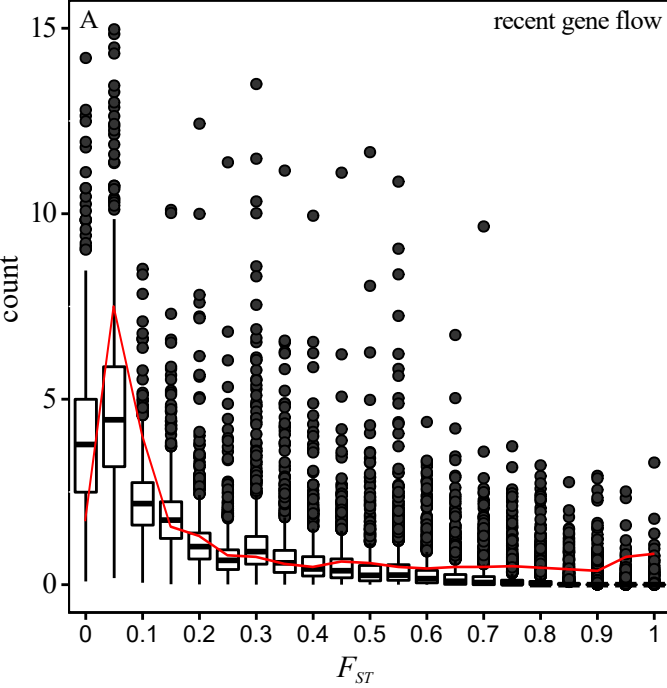
AGF 0.23

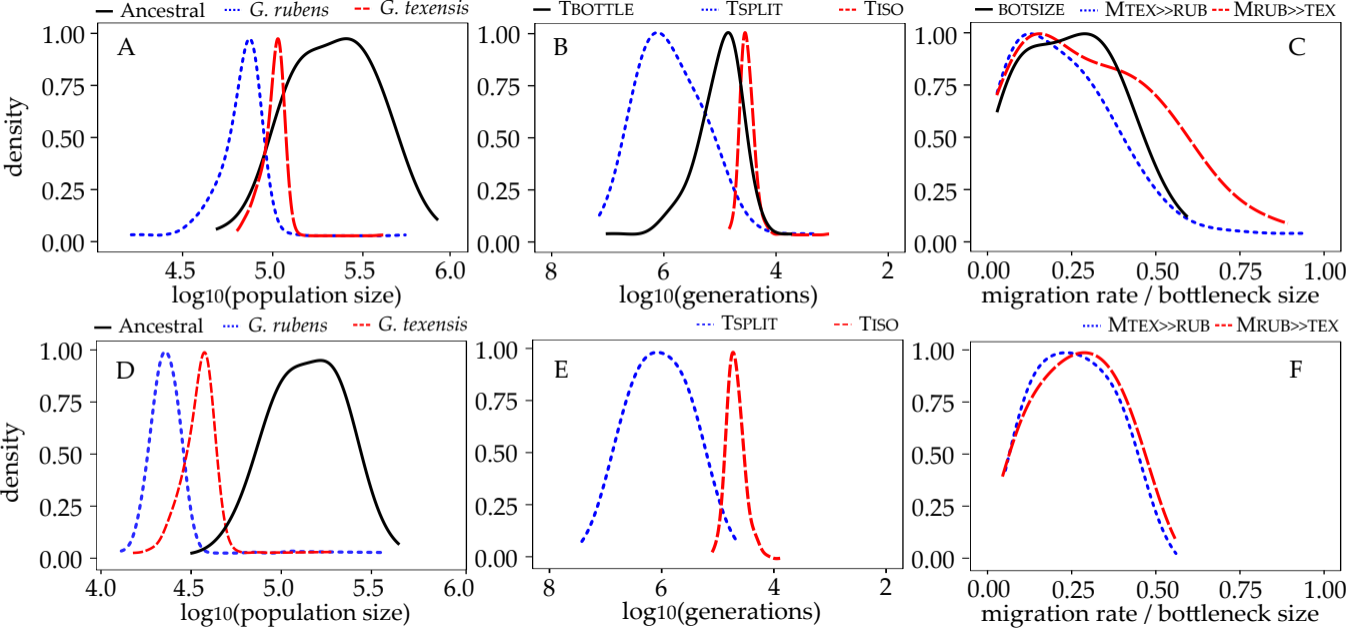
RB 0.00

AGFRB 0.77









Populations

bioRxiv preprint doi: <https://doi.org/10.1101/193828>; this version posted December 20, 2017. The copyright holder for this preprint (which was not certified by peer review) is the author/funder, who has granted bioRxiv a license to display the preprint in perpetuity. It is made available under aCC-BY-NC-ND 4.0 International license.

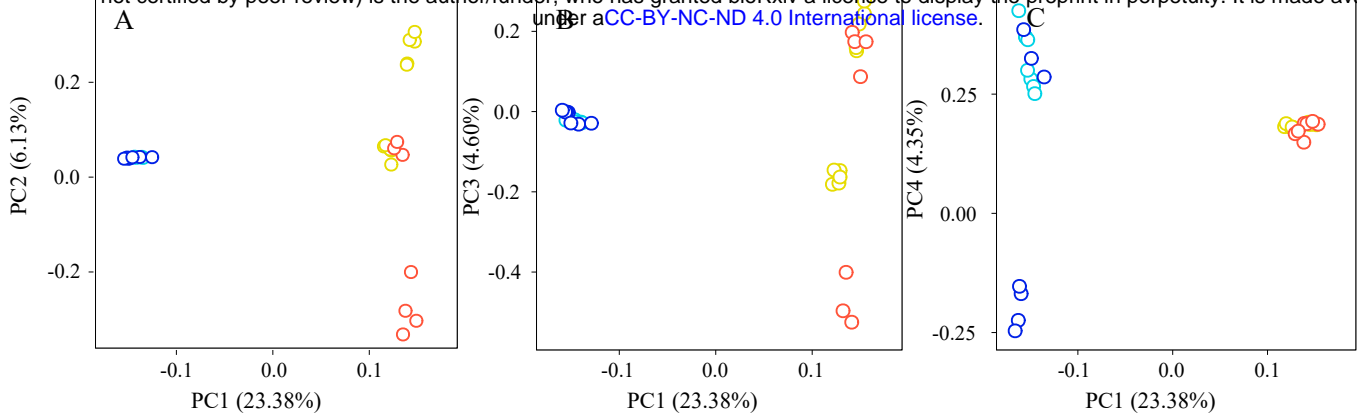


Fig S1. Population substructure in *G. rubens* and *G. texensis*. Variation in allele frequencies between species and between populations within species (Lake City and Ocala for *G. rubens*; Lancaster and Austin for *G. texensis*) is shown. The allele frequency variation in all 175,244 SNPs is summarized in the first four principal components teasing apart the species (PC1), and the populations in *G. texensis* (PC 2) and *G. rubens* (PC 4). Note that clustering along the PCs explaining within species variation among populations is much weaker compared to clustering of the species along PC1.

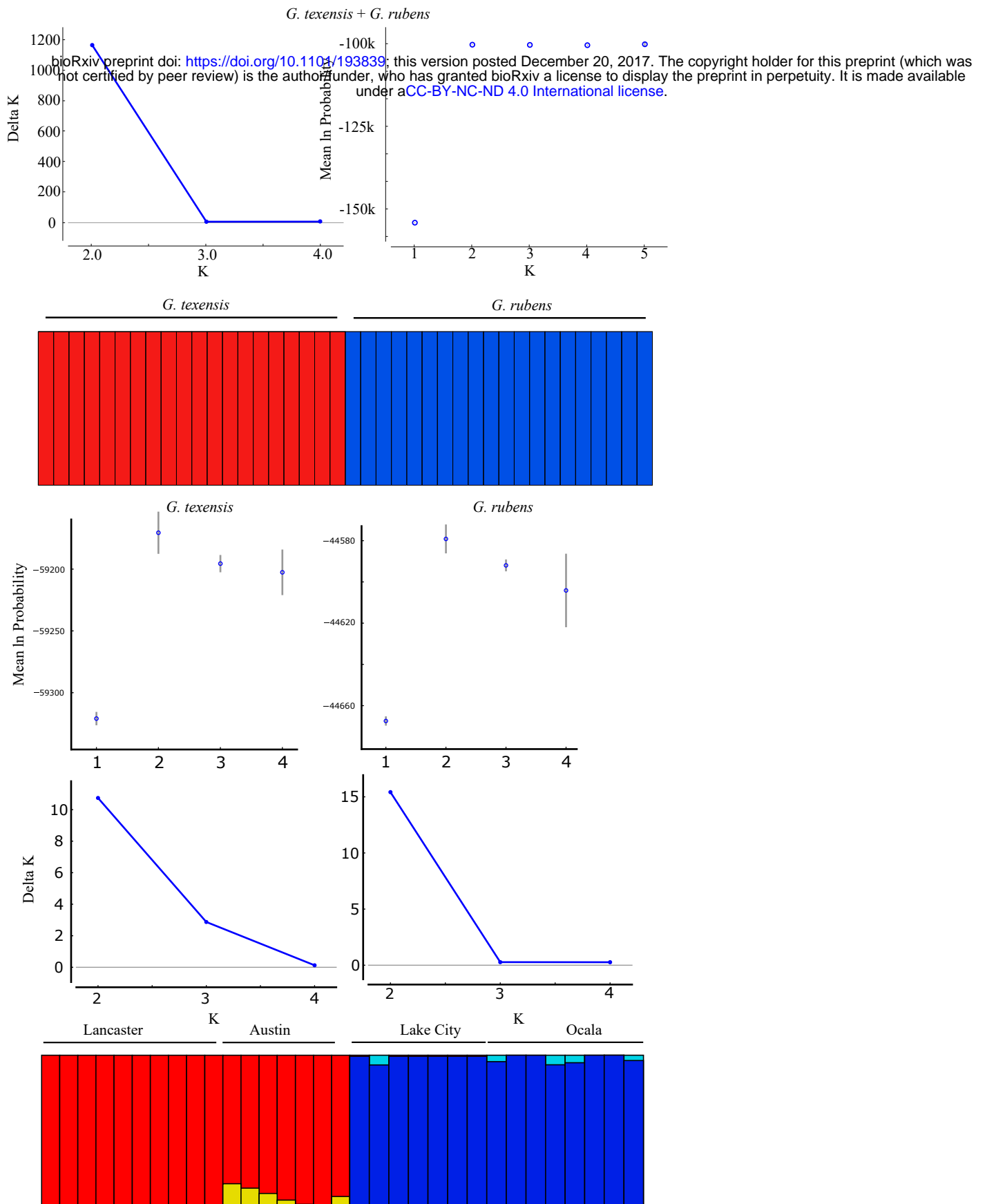


Fig S2.STRUCTURE results. For each of the species, STRUCTURE was run for 100,000 iterations at values for K=1 through K=4 (K=5 for the species combined). The mean natural logarithm of the probability and the delta K (increase or decrease in likelihood between consecutive runs for different values of K) were inspected to determine the most likely predicted number of populations. A run of *G. rubens* and *G. texensis* separately showed in both cases that, although the highest likelihood was for K=2, differences with K=1 were only marginal and a defined pattern in population substructure was absent (see also the bar plots at the bottom). The run for the species combined (K=2) shows no introgression of *G. texensis* genes into the *G. rubens* or vice versa.

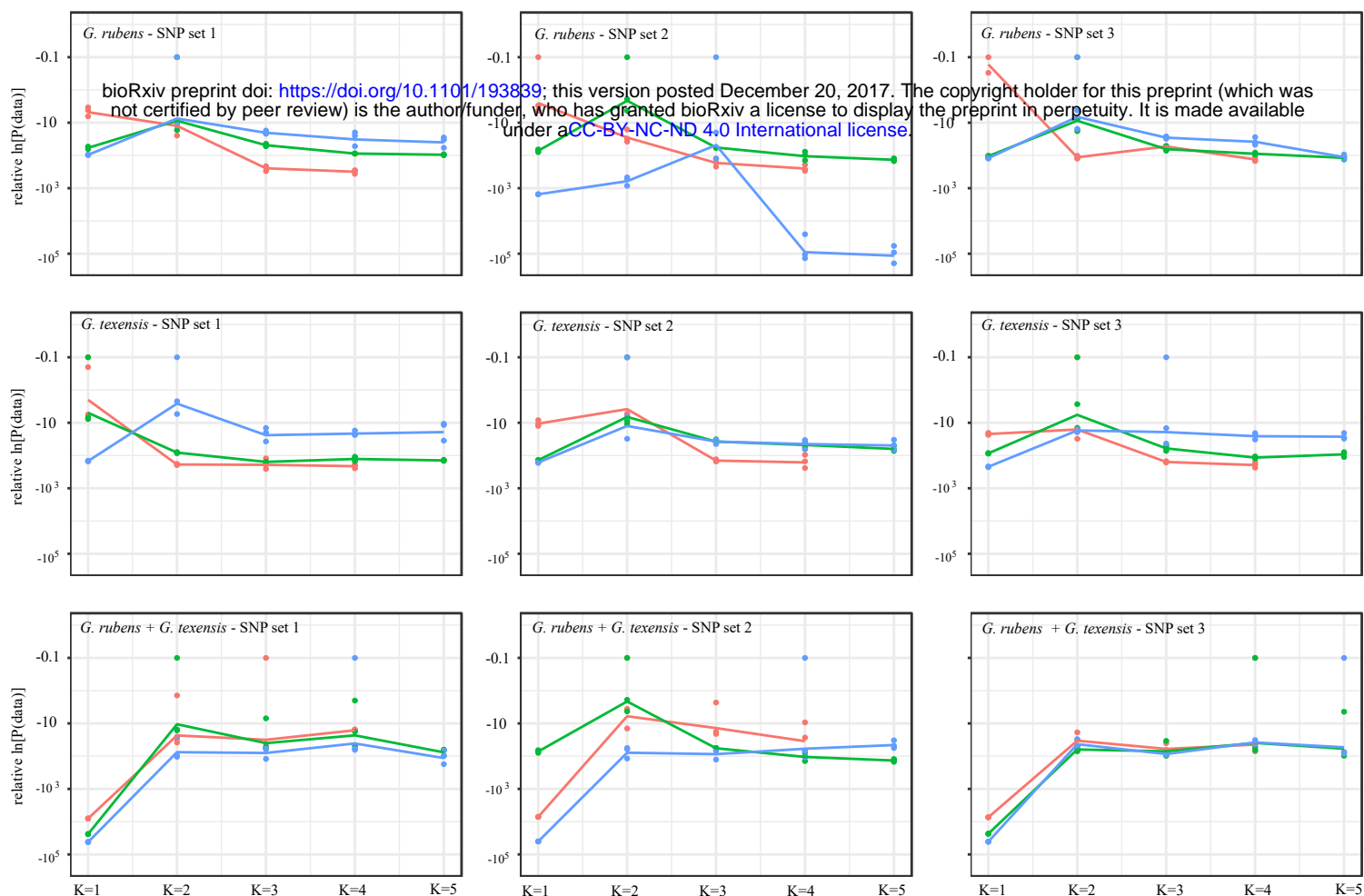


Figure S3. Relative natural log transformed probability of the data under different values for K. The raw probabilities from STRUCTURE relative to the maximum probability is shown for each K, for three random sets of 8835 SNPs (one per contig), and for *G. rubens*, *G. texensis*, and for the species combined (excluding eight individuals to correct for cryptic relatedness). Within each panel, the dots show each of the three iterations and the lines show the trend in the average difference in probability with the maximum probability for three different sample sizes: two random individuals per population (red), five random individuals per population (green), and all the individuals sampled from the populations.

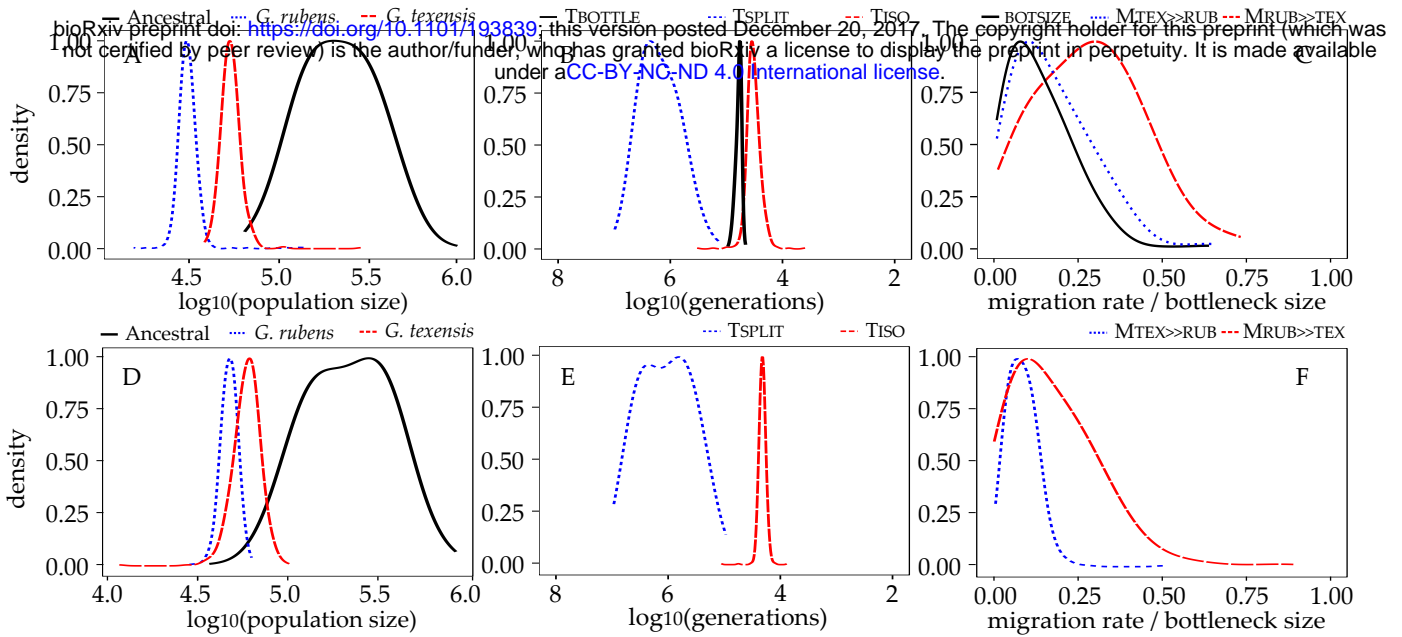


Fig S4. Demographic parameter estimation for the model with all 40 individuals. For the AGFRB (A-C) and the AGF models (D-F) the density distributions of the the ancestral and current population sizes (A,D), the time since divergence, cessation of gene flow, and recovery to current population sizes after the bottleneck (B,E), and the migration rates and bottleneck size (C,F) are shown. The density lines have been trimmed to the existent parameter distribution (i.e., no density extrapolation) and have been smoothed by adjusting the bandwidth. For lines within one panel the same smoothing bandwidth has been used.



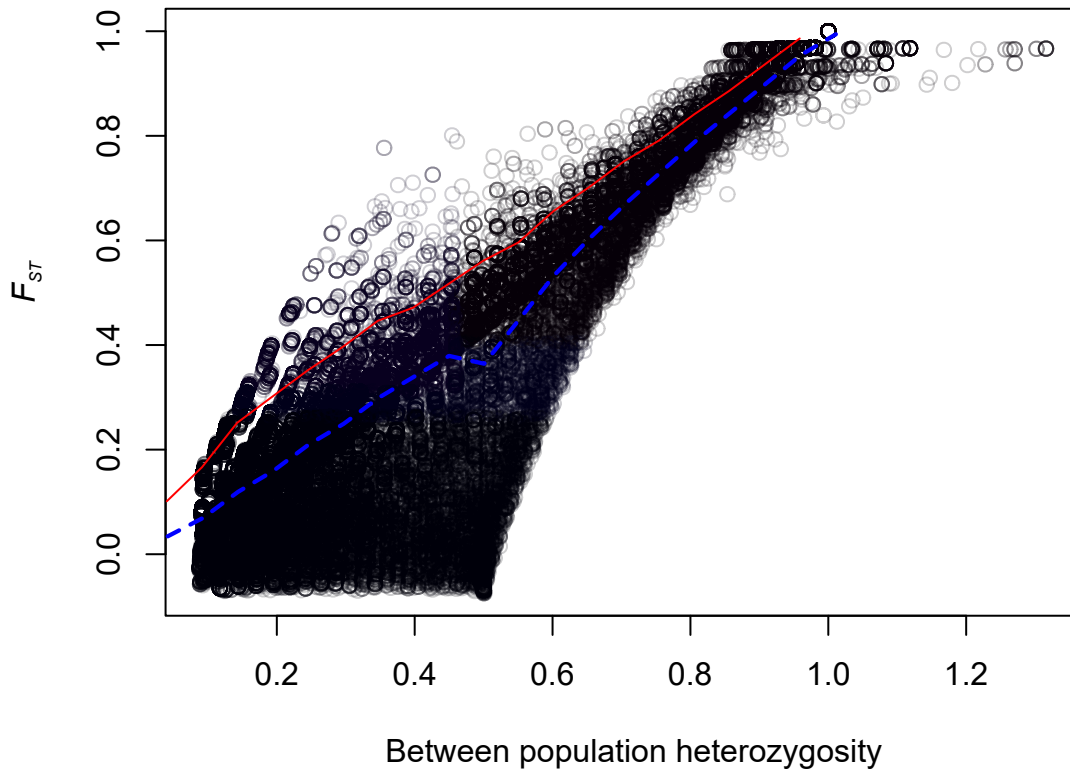


Fig. S5. Arlequin  $F_{ST}$  based selection scan. The circles represent estimates for the  $F_{ST}$  and between population heterozygosity for all SNPs with  $MAF > 0.05$  (81,125 SNPs). The blue dashed and red solid line are the median and 99th quantile, respectively, of the simulated null distribution for this relationship under a hierarchical island model. Any SNPs above the red solid lines were considered outliers.